Anthropogenic Climate Change Drives the Melting of Glaciers in the Himalaya

Shakil A Romshoo (shakilrom@kashmiruniversity.ac.in)
University of Kashmir https://orcid.org/0000-0003-0070-5564
Khalid Omar Murtaza
University of Kashmir
Waheed Shah
University of Kashmir
Tawseef Ramzan
University of Kashmir
Ummer Ameen
University of Kashmir
Mustafa Hameed Bhat
University of Kashmir

Research Article

Keywords: Glacier dynamics, Climate change, Greenhouse Gases, Dass Ladakh, Western Himalaya

Posted Date: December 28th, 2021

DOI: https://doi.org/10.21203/rs.3.rs-1112748/v1

Version of Record: A version of this preprint was published at Environmental Science and Pollution Research on March 10th, 2022. See the published version at https://doi.org/10.1007/s11356-022-19524-0.

Abstract

The Himalayan glaciers supply water to a large population in south Asia for various uses and ecosystem services. Therefore, regional monitoring of glacier melting and identifying the drivers thereof is important to understand and predict the future trends of cryospheric melting. Using multi-date satellite images from 2000-2020, we investigated the shrinkage, snout retreat, thickness changes, mass loss and velocity changes of 77 glaciers in the Drass basin, western Himalaya, India. The overall glacier cover has shrunk by 5.31±0.33 km^2 during the period. Snout retreat varied between 30-430 m (mean 155±9.58 m). Debris-cover showed a significant influence on the glacier melting with the clean glaciers showing a higher loss of ~5% compared to the debris-covered glaciers (~2%). The glaciers on an average have shown thickness change and mass loss of -1.27±0.37 and -1.08±0.31 m w.e.a^{-1} respectively. Average glacier velocity has reduced from 21.35±3.3 m a^{-1} in 2000 to 16.68±1.9 m a^{-1} by 2020 due to the continuous melting and the consequent mass loss of the glaciers. Concentration of the greenhouse gases (GHGs), black carbon and other pollutants from vehicular traffic plying in the vicinity of the glaciers has significantly increased during the observation period. Increasing temperatures, result of the significant increase of the GHGs and pollutants in the atmosphere, drive the glacier melting in the study area. If the situation continues in the future, the glaciers may disappear altogether in the Himalaya leading to significant impact on the regional water supplies, hydrological processes, ecosystem services and transboundary sharing of waters.

Introduction

Cryosphere constitutes an important components of the Earth's natural system particularly in the Himalaya (Lemke et al. 2007; Barry and Gan 2011) also called as the world's 'third pole'. Although mountain glaciers constitute only ~3% of the worldwide glacial area (Arendt et al. 2002), the necessity for precise areal and volumetric estimations of mountain glaciers is well established, as they constitute the important freshwater reserves and contribute immensely to meet the water demands of a large population of people in the south Asia and other neighbouring countries (Kääb 2005; Immerzeel et al. 2010). Melting of the Himalayan glaciers also contributes to the sea-level rise and increasing frequency of glacier hazards like GLOFs (Glacial Lake Outburst Floods), avalanches, landslides and permafrost creep due to their sensitivity to climate change (Kääb et al. 2006; Debella-Gilo and Kääb 2011; Snehmani et al. 2014; Veh et al. 2019; Thompson et al. 2020; Khan et al. 2021). Therefore, continuous monitoring of glacier recession and dynamics is important for observing the direct impacts of climate change on water security, water supplies, future sea levels, and glacier-related disasters.

One of the notable impacts of climate change in the Himalaya is the significant glacier thinning and melting (Shrestha and Aryal 2011; Ali et al. 2021; Dixit et al. 2021). However, the observed thinning and melting is characterized by heterogeneity across the Himalaya (Abdullah et al. 2020; Sakai and Fujita 2017; Farinotti et al. 2020). To understand and explain the heterogeneous glacier response, the influence of climate change, glacier morphology and local topography, and other influencing factors has been extensively investigated (Fujita and Nuimura 2011; Garg et al. 2017; Murtaza and Romshoo 2017; Sam et

al. 2018; Abdullah et al. 2020). Several studies have estimated the two-dimensional (i.e. glacier area, length, or snout) glacier changes (Cogley 2011; Zemp et al. 2015; Romshoo et al. 2020) which represents an assessment of indirect, delayed, and filtered response of changing climate (Scherler et al. 2011; Gardelle et al. 2013; Bhattacharya et al. 2016). Most of the studies have reported the general state of glacier recession during the past few decades across the Himalaya except for some portions in the Karakoram where glaciers have showed advance, surge, irregular behaviour and even retreat (Ren et al. 2006; Bhambri et al. 2011; Bolch et al. 2012; Paul 2015; Chand and Sharma 2015; Murtaza et al. 2021).

However, studying other parameters along with the two-dimensional change like glacier surface ice velocity, elevation and mass balance changes of glaciers to assess their overall dynamic response to changing climate is now widely promoted (Gardelle et al. 2013; Vijay and Braun 2016; Shukla and Garg 2020). Glacier mass balance and thickness changes show the direct influence of climate change on glacier melting and the consequent changes in the streamflow. Similarly, glacier velocity is a useful measure for assessing the changes in glacier ice thicknesses, mass changes, glacier advance and retreat, and glacier ice flow regimes (Tiwari et al. 2014; Singh et al. 2021). Unfortunately, only a few mass balance, glacier thickness and glacier velocity studies have been conducted at basin or range scale in the Himalaya (Dehecq et al. 2019; Gardelle et al. 2013) and this shortcoming constraints the understanding of glacier response to climate change in the Himalaya. The inadequate and even sometimes lack of the observations of the driving factors of the glacier melting related to climatic, hydrological and atmospheric processes further complicates the understanding of cryospheric melting in the data-scarce Himalaya.

In line with the global glacier recession trend, the glaciers in the Drass region of the Western Himalaya have receded since Late Holocene (Koul et al. 2016; Rashid et al. 2021). Although a few studies have estimated the recession of glaciers in this region in terms of area loss, snout retreat and glacier length changes, particularly focused on one glacier, the Machoi Glacier (Koul et al. 2016; Rashid et al. 2021; Pall et al. 2019) but overall the glacier dynamics and impacts of climate change on glaciers in Drass region has not been investigated comprehensively, and therefore the role of the controlling factors on the observed glacier recession remains unknown. This study related the observed glacier shrinkage, snout retreat, changes in glacier thickness, mass loss and velocity estimates of the glaciers in the Drass region, based on Landsat images, topographic maps, SRTM 30 and TerraSAR-X/TanDEM-X acquisitions, with the observed changes in the greenhouse gas emissions, pollutants, temperature and precipitation trends obtained from various sources, in order to understand the influence of controlling factors driving glacier recession in the study area.

Study Area

The gateway to the cold desert valley of Ladakh and the 2nd coldest inhabited place in the world, Drass is located in north-western part of Himalayas, nearly 140 km from Srinagar, Kashmir (Figure 1). The Drass Valley begins from the base of the Zojila Pass, en-route to Ladakh, stretching from 34.10° to 34.45°N and 75.10° to 76.05°E with an elevation range of 2705-5942 m. Drass is surrounded by Greater Himalayas and Drass Mountains and is regarded as one of the finest tourist hubs for its high altitude trekking routes

and tourist sites in the region. The high relief and overall steepness of slopes provide an overwhelming impression that region has distinct climatic and geomorphic setting. Geologically, the major portion of the area is characterized by Drass volcanics, Triassic-Jurassic Limestone, Salkhala, and other geological formations, viz., Ladakh Plutonic Complex, Lamayuru and Kargil (Liyan, Kailas), occupying only a small portion of the region (Thakur and Rawat 1992).

Drass valley has cold semi-arid type of climate and receives precipitation in the form of snowfall during winter season from the Western Disturbances and rainfall during summer season from both the Westerlies and Southern Jet stream Movements (Koul et al. 2016). Although the glaciers are distributed throughout the region, however a major chunk of the glaciers are present around the southern portions of the region. Machoi Glacier (G35) is one of the major glacier in the study area, which is easily acceded from the Srinagar- Ladakh national highway. Various glacial landforms, viz., U-shaped valleys, arêtes, erratic boulders, lateral moraines, and terminal moraines are well preserved in the study area. However, moraines are the dominant landforms preserved across the region. The presence of the abundant erosional and depositional glacial landforms in the study area indicates that the area has been significantly glaciated in the recent past.

Materials And Methods

Satellite Data

In this study, a host of snow- and cloud-free satellite data from various sensors was used for glacier area changes, snout changes, velocity measurements, glacier thickness and mass change and greenhouse gases (Table 1). Landsat ETM+ and OLI satellite images, acquired at the end of the ablation season, were selected for glacier area and snout retreat mapping, because this period is usually cloud-free and there are almost no snow packs in the valleys adjacent to glaciers (Kääb 2002; Paul et al. 2002). Further, panchromatic images of ETM+ (1999-2000) and OLI (2019-2020) were used for the glacier velocity estimations. The Shuttle Radar Topography Mission (SRTM) DEM was used to generate various glacier morphological and topographical parameters. SRTM 30 and TanDEM-X acquisitions were used for estimating glacier thickness changes. Further, in order to estimate the greenhouse gases (GHGs) trends over the study area, the satellite data from the Atmospheric Infra-Red Sounder (AIRS), Greenhouse gases Observing Satellite (GOSAT), and Ozone Monitoring Instrument (OMI) were used. The vehicular data plying on the national highway passing through the study area, during 2010-2020 period, was obtained from the Traffic Department, Government of Ladakah. To ascertain the long-term climate trends in the study area, mean annual temperature and precipitation derived from Climatic Research Unit (CRU) time series (TS) v-4.04 grids of dimension 0.5° x 0.5° (Harris et al. 2020) was used.

Glacier shrinkage and retreat mapping

Remote sensing methods are helpful for mapping and monitoring spatial and temporal changes of glaciers (Racoviteanu et al. 2008; Bajracharya et al. 2014). Although field-based monitoring is required to study the glacier parameters such as the extent, snout position, glacier depth, and mass balance,

however, it is extremely challenging, labour intensive, and time consuming, especially for the mountainous regions like the Himalaya with harsh climatic conditions, rugged terrain, security challenges and remoteness (Gao and Liu 2001; Murtaza and Romshoo 2014). Visual image interpretation and digital image processing of the satellite data using various algorithms were used for mapping glacier outlines (Paul et al. 2002; Murtaza et al. 2021). Compared to the accumulations area, major changes usually occur in the ablations area of a glacier below the equilibrium line altitude (ELA) (Paul et al. 2017; Shukla et al. 2020), therefore, we restricted the glacier area mapping and change detection analysis to the ablation zone below the ELA. Glacier snout was delineated based on the presence of certain characteristic features such as ice wall, proglacial lakes and emergence of streams from the snout (Murtaza and Romshoo 2017). Google Earth imageries were used to check the accuracy of glacier boundaries wherever available.

Topographical characterization

Influence of the local morphology and topographic parameters on glacier recession was analysed in this study. Influencing factors viz. glacier size, altitude, and slope were analysed to understand the heterogeneous behaviour of glaciers. Various studies have reported significant influences of local topographic parameters on glacier recession (Bolch et al. 2012; Murtaza and Romshoo 2017; Romshoo et al. 2020). Based on the glacier size, the glaciers were categorized into three classes, viz., small (0.27-1.00 km^2), medium (1-5 km^2), and large (5-14 km^2) glaciers. Based on the altitude, the glaciers were categorized into three categories such as; the glaciers between 4600-5000 m, glaciers between 5001-5400 m, and glaciers between 5401-5800 m. Similarly, on the basis of glacier slope, glaciers were classified into two slope categories; glaciers with gentle slope (<15°) and those with steeper slopes (>15°).

Debris cover Mapping

Debris-covered part of the glaciers was identified visually using slope and thermal characteristics of the glaciers from the Landsat images and was delineated using onscreen manual digitization technique in GIS environment (Dobhal et al. 2013; Shukla and Garg 2019). We considered only areas with a fairly continuous debris-cover extent over the glaciers and discarded the small isolated patches of debris present sporadically over the glaciers from the debris-cover mapping. Spatio-temporal changes in the supra-glacier debris-cover exert significant influence on glacier recession. Thus, in order to understand the role of debris-cover over the glacier recession, the glaciers in the study area were categorized into clean glaciers (CGs) having less than 5% debris-cover and debris covered glaciers (DCGs) having more than 5% debris-cover.

Surface Ice Velocity (SIV) measurement

39 glaciers with size more than 1 km2 were selected from the study area for the SIV estimations as the small glacial morphological features are not identifiable on the glaciers using Landsat images (Shukla and Garg 2020). Observations of earth's surface features using remotely sensed data along with the feature tracking method have proved useful in monitoring velocity of a glacier (Scherler et al. 2008; Wu et

al. 2020; Zhao et al. 2020). SIV was calculated using the Co-registration of Optically Sensed Images and Correlation (Cosi-Corr) approach based on the use of repeat orthorectified snow- and cloud-free Landsat ETM+ and OLI images acquired at the end of ablation season between 1999/2000 and 2019/2020. Cosi-Corr is a Fourier-based highly sophisticated matching algorithm for the detection of co-seismic displacements (Leprince et al. 2007) which offers sub-pixel accuracy and has been widely used by researchers to measure glacier displacements mainly for push-broom sensors (Heid 2011; Scherler et al. 2011; Tiwari et al. 2014; Sahu and Gupta 2019; Shukla and Garg 2020). The SIV calculations using Cosi-Corr algorithm employs three processes orthorectification, co-registration and correlation and the details of the algorithm is described by Scherler et al. 2008. Before computing the SIV, the displacement images were checked and modified for different possible errors and several filters were applied. Initially, low signal to noise ratio (SNR) values less than (0.9) filtered to remove the poorly correlated pixels. Because of the some poorly correlated pixels, the SIV values >200 m a-1 were also removed to exclude the flawed values SIV values (Bhattacharya et al. 2016; Bhushan et al. 2018).

Landsat images have high spatial and temporal coverage (Ding et al. 2016; Shukla and Garg 2020) but have subpixel noise formed by attitude variations (Heid and Kääb 2012; Bhattacharya et al. 2016). The average image-to-image registration precision for ETM+ and TM sensors is ~5 and ~6 m (Storey and Choate 2004; Bhattacharya et al. 2016), which is, because of their whisk-broom nature, which is difficult to model. However, this precision is justified for glaciological studies (Heid and Kaab, 2012).

Glacier mass changes

The glacier thickness change were estimated based on the elevation differences in the SRTM DEM (2000) and TanDEM-X (2012-2015) obtained ~12 year apart. In order to remove the horizontal and vertical offset between the two DEMs, the universal co-registration algorithm was used (Nuth and Kääb, 2011). The co-registered DEMs were differenced to generate the elevation difference (dH/dT) map over the glaciated terrain. The DEMs were corrected for radar penetration bias before generating the DEM difference map at pixel level. Using the density conversion factor of 850 kg m^{-3}, the volume changes were then converted into glacier mass changes. The detailed procedure for glacier elevation changes and mass thickness is described in Abdullah et al. 2020.

Vehicular traffic and BC data analysis

In order to assess the direct impacts of the vehicular movement on glcier shrinkage and recession in the study area, the glaciers were grouped into two categories on the basis of their proximity to the National Highway (NH) by creating a buffer of 6 km^2 on either side of the highway i.e. proximal glaciers situated within the 6 kms buffer from the NH and distant glaciers situated outside the buffer zone.

The vehicle data, in terms of light and heavy motor vehicles plying daily on the national highway, obtained from Traffic department, Ladakh government, was analysed for the emission quantities of the GHGs and particulate pollution. The main fuel used by the vehicles is petrol and diesel. Emission factors (EFs) were calculated by adopting the methodologies prescribed by various researchers for different

gases and particulate matter (Baidya et al. 2009; Prakash et al. 2018; Ramachandra et al. 2015; Richardson 1999) and the estimation depends on the age, engine technology, and the type of fuel by the vehicles. Emissions from road traffic were estimated based on the number of vehicles and distance travelled by the vehicles in a year (Ramachandra et al. 2015).

Black carbon, the main constitutent of the vehicular pollution was measured in the study area on the ablation zone of one of the glacier site, viz., Machoi Glacier during one of the field expeditions conducted from 29 Sep to 03 Oct 2014 for about 9-10 hours daily using the portable AE-42 Athalometer (Magee Sci., Inc., Berkeley, CA, USA) (Bhat et al., 2017). However, the area averaged Black Carbon (BC) surface mass concentration for a longer period during 1980-2020, available from the Modern-Era Retrospective Analysis for Research and Applications (MERRA) at a spatial resolution of 0.5˚ x 0.625˚, was also used to determine the long-term changes in BC in the study area.

Climate change data analysis

To ascertain the long-term climate trends in the study area, at time series of mean annual temperature and precipitation derived from Climatic Research Unit (CRU) time series (TS) v-4.04 grids of dimension 0.5° x 0.5° was used (Harris et al. 2020), as the meteorological observations over the area are very scarce due to the challenging rugged topography, remoteness and harsh climatic conditions. The time series of the data from 1901-2019 was analysed statistically using the non-parametric Mann-Kendall test to determine the significance of the trends in the data (Mann 1945; Kendall 1975). The time series climate data was grouped into three bins; 1901 to 1940, 1941 to 1980 and 1981 to 2019 because of the presence of three distinct periods showing specific climate trends. The influence of climate change on glacier recession was assessed by comparing climate data trends with the observed recession in the study area.

Greenhouse gas data analysis

In order to assess the trend of greenhouse gases (GHGs) and their impact on glacier shrinkage and recession in the study area, we examined the temporal trends of CO_2, O_3, NO_2, CH_4, and atmospheric water vapour using a time series of satellite data, of varying period during 2002-2020, from the GOSAT, AIRS, and OMI satellites (Table 1). The satellite data used for retrieval of O_3 data from January 2003 to December 2020 data is from the gridded AIRS version 6, monthly weighted means, level 3 product, referenced as AIRX3STM v006 (CHAHINE et al. 2006). GOSAT satellite data was used for retrieval of CO_2 column density from January 2009 to December 2019. The data has a relative accuracy of 1%, which is about 4 ppm for CO_2 and accuracy of 2% a spatial scale of Î (Kuze et al. 2009). The satellite data used for retrieval of CH_4 data from January 2003 to December 2020 data is from the gridded AIRS version 6, monthly weighted means, level 3 product, referenced as AIRX3STM v006. AIRS channels around 7.6µm are used for CH_4 retrieval, based on the atmospheric temperature and water moisture profiles, and surface temperature and emissivity (Kramer et al. 2021). NO_2 columnar was retrieved from OMI (Ozone Monitoring Instrument) level 3 daily global gridded (0.25° x 0.25°) (OMNO2d) data and comprises of the total tropospheric Column NO_2, for all atmospheric conditions. However, for sky conditions where cloud

fraction is less than 30%, visible channel was used for NO_2 retrieval (Krotkov et al. 2016). Columnar water vapour retrieved from AIRS version 6-product referenced as, AIRS3STD.V006 from January 2003 to December 2020. AIRS water vapour product presents a standard physical retrieval that includes both AIRS and AMSU radiances (used for cloud clearing)(Susskind et al. 2003).

Accuracy assessment

Glacier recession

The study involved extraction of various glacial parameters utilizing multi-temporal satellite data with variable characteristics; hence, it is important to quantify the uncertainties associated with mapping the glacier outlines based on the use of satellite data. The errors due to the use of multi-temporal satellite data arise from the positional and mapping errors. Uncertainty of glacier mapping depends on the resolution of the imagery used and the prevailing conditions at the time of image acquisition. Under the best conditions, an accuracy of less than half a pixel can be achieved (Bolch et al. 2010; Murtaza et al. 2021). The error due to the use of variable resolution satellite data was eliminated using the Landsat satellite images having the same resolution. The buffer method suggested by Bolch et al. (2010) and Granshaw and Fountain (2006), was used for assessment of the uncertainties in the glacier area mapping. A buffer width, half of the pixel resolution of the source image, was used for the uncertainty assessment. The glacier terminus change uncertainty (U) was estimated as suggested by Hall et al. (2003) as:

$$U = \sqrt{a^2 + b^2} + \sigma$$

where a and b is the spatial resolution of the two satellite images used for glacier mapping and σ represents the error in image registration.

Glacier velocity

The lack of field-observed glacier velocity measurements hinder the accuracy assessment of the remotely sensed SIV measurements. Quality of the remote sensing derived SIV is mainly hampered by the; image quality (snow- and cloud-cover), pre-processing (ortho-rectification, co-registration), the matching method itself and the transformation of the surface between the two image acquisitions (Scherler et al. 2008; Heid and Kaab 2012; Bhushan et al. 2017). To reduce the errors owing to image quality, it was made sure that the images used for SIV have minimal snow- and cloud cover and were acquired towards the end of ablation season (Paul et al. 2015). The uncertainty from the pre-processing and matching method are usually the simplest errors to overcome (Scherler and Strecker 2012). Orthorectification rectifies the horizontal shifts that are not because of the displacement but due to the errors associated with the base DEM used in the process. The uncertainties in the SIV from the DEM can be minimized if the correlated images are acquired from the same path and row (Heid and Kaab 2012). Since the Landsat images are already co-registered, therefore the error is negligible and lies within the limits required for glaciological

studies (Storey and Choate 2004; Heid and Kaab 2012; Bhattacharya et al. 2016). The image correlation accuracy is of the order of 1/20–1/10 of the pixel size which would imply an error of about ±1.5 m a^{-1} (Tiwari et al. 2014). The error due to transformation of the surface between the two image acquisitions is difficult to quantify because of the deformation, melting, opening or closing of crevasses and spatial distribution of debris-cover on glacier and therefore persists as a residual error (Shukla and Garg 2020). The total uncertainty in the SIV estimates was calculated as per the approach given by Scherler and Strecker 2012 and Garg et al. 2017 assuming that the SIV over the non-glaciated terrain is zero. The mean standard deviation ($\sigma_{\text{stable area}}$) and mean velocity over the non-glaciated stable area ($M_{\text{stable area}}$) were summed up and divided by the time span between the correlated images.

Results And Discussion

Glacier area changes

In all, 77 glaciers were identified and mapped in the Drass region using Landsat imageries of 2000 and 2020 (Figure 2). The size of the glaciers ranges from 0.27 to14.01 km^2 with the average size of 2.30 km^2. It was observed that the glacier area in the region has reduced from 176.77±10.70 km^2 in 2000 to 171.46±10.37 km^2 in 2020 showing a loss of 5.31±0.33 km^2 (3%) during the last two decades. However, the rate of glacier recession is heterogeneous among the glaciers and ranges between 0.24% (G57) to 15% (G15), with the average recession rate of ~5% (Table S1) controlled primarily by varying size and topographic parameters like elevation, slope and aspect of the glaciers. Overall, the glacier cover in the study area has reduced by 0.26 km^2 yr^{-1} during the last 20 years.

Despite being one of the important resource of water with numerious uses, the glaciers in the North Western Himalaya has been grossly under-studied compared to the neighbouring areas of the Himalaya. Apparently a few studies regarding to the glacier recession has been caried out till date in the study area (Koul et al. 2016; Rashid et al. 2021). Koul et al. 2016 studied 81 glaciers in the region using SOI topographic map of 1976 and LISS-III imageries of 2001 and 2013. They suggested that the glaciers have receeded from 187.9 km^2 in 1965 to 156.65 km^2 in 2013, primarliy owing to the differences in morphology, topography and climate change. Rashid et al. 2021 recently studied Machoi Glacier in the Drass region and reported a recession of 29% (0.62% yr^{-1}) from 1972 to 2019. The comparisions of the results of glaciers recession observed in this study with the previous studies (Chudley et al. 2017; Romshoo et al. 2020; Shukla et al. 2020) revealed that the recession rate of Drass glaciers is in line with the glaicer recession rate of other adjacent glaciated regions with some minor variations (Table 2) primarily due to the differences in the observation period, datasets used and number of glaciers investigated.

Influence of topographic and morphological factors on glacier recession

Glacier recession indicates the declining health of the glaciers in the study area during the observation period. However, the rate of glacier recession varies primarily because of the variable climatic and non-

climatic parameters in the study area. Various studies have highlighted the significance of the topographic and morphological parameters on glacier recession in the Himalaya (DeBeer and Sharp 2009; Jiskoot et al. 2009; Scherler et al. 2011; Bolch et al. 2012; Murtaza and Romshoo 2017). Therefore, the impact of topographic and morphological parameters like; size, altitude, and slope on the glacier recession has been assessed and is discussed below;

Influence of glacier size on recession

Several studies have emphasized the size dependency of glacier recession (Diolaiuti et al. 2012; Romshoo et al. 2020; Shukla et al. 2020). Based on the size, the glaciers were categorized into three classes, viz., small (0.27-1.00 km^2, N=29), medium (1-5 km^2, N=40), and large (5-14 km^2, N=8) glaciers (Table 3). The analysis revealed that small glaciers have lost ~8% of the area, medium glaciers have lost ~4% and the large glaciers have lost ~2% of the area. It is evident from the analysis that small glaciers have shrunk more as compared to the medium and larger glaciers, a fact corroborated from other regions of the Himalaya (Bhambri et al. 2011; Schmidt and Nüsser 2012; Das and Sharma 2019). The small glaciers are more sensitive to changing climate than the larger ones, because of their faster response time compared to the larger sized glaciers and is dependent on glacier thickness (Oerlemans and Fortuin 1992; Huss and Fischer 2016).

Impact of altitude on glacier recession

Glaciers in the study area occur within a wide elevation range from 3600 to 6700 m with most of the glaciers situated between 4600-5800 m. Although, glaciers across all the elevation ranges are receding, but the recession varies along the elevation gradient. Based on the altitudinal situation, the glaciers were categorized into three categories such as; the glaciers between 4600-5000 m, glaciers between 5001-5400 m, and glaciers between 5401-5800 m (Table 4). Analysis of the glacier recession w.r.t. elevation suggests that the glaciers situated at the lower elevations have receded by 4.10% compared to the glaciers at the mid and higher elevations showing a lower recession of 3.23% and 1.46% respectively during the observation period. The general observed trend indicates that the glaciers located at relatively higher elevation experience lower temperature, and receive higher amount of snow precipitation and therefore experience less ablation or even mass gain. The results are thus in line with the normal behaviour of recession with respect to the elevation. Various studies have reported significant altitudinal influences on glacier recession with the glaciers located at lower elevations tending to recede faster and vice-versa (Hewitt 2005; Fujita and Nuimura 2011; Venkatesh et al. 2012; Kumar et al. 2021).

Impact of slope on recession

Several studies have highlighted the influence of topographic slope on glacier recession (Venkatesh et al. 2012; Nainwal et al. 2016). Slope affects ice velocity, mass flux, and snow accumulation rates through its effect on avalanche transportation of snow over the glacier surface (Hoelzle et al. 2003). Glaciers in the study area have slopes in the range of 11° to 28.5° with the mean slope of 18°. To evaluate the influence of slope on glacier recession, glaciers were classified into two slope categories (Table 4); glaciers with

gentle slope (<15°) and those with steeper slopes (>15°). It was observed that the glaciers with gentle slope (<15°) have experienced a lower recession of 2.30% compared to the recession of 3.60% shown by the glaciers having steeper slope (>15°). However, these results are contrary to those reported in various other studies (Venkatesh et al. 2012; Patel et al. 2018; Shukla et al. 2020). The reason for the higher recession rate shown by the glaciers situated at steeper slopes is possibly due to their mean lower elevation, as the glaciers situated at lower elevations are susceptible to higher ablation rates (Fujita and Nuimura 2011; Pandey and Venkataraman 2013; Murtaza et al. 2021).

Snout recession

Analysis of the data from 2000 to 2020 showed that the snouts of all the glaciers in the study area have retreated, however the retreat rates show considerable variation among the glaciers. The snout retreat varied from 30 m to 430 m with the average snout retreat of 155 ±9.58 m during the period (5.75 ±0.47 m a^{-1}). Further, from the analysis of the snout recession data, it was observed that the larger glaciers (5-14 km^2) are showing higher annual snout retreat rate (10.55 ±0.47 m a^{-1}) than the smaller glaciers (6.81 ±0.47 m a^{-1}) (Romshoo et al. 2020).

Debris cover changes

The glaciers in the study area have varying extent of debris cover ranging from 0.10 to 2.12 km^2 (Figure 3). The variation in the debris cover of the glaciers situated within the same geographic setting is either due to the differences in the surrounding lithology or varying geomorphic setting (Scherler et al. 2011). Temporal analysis showed that the debris-cover of the glaciers has increased from 11.10 km^2 in 2000 to 14.20 km^2 in 2020, showing an increase of 28% during the period (0.15 km^2 yr^{-1}). The results are in general agreement with the past studies conducted in various other regions of the Himalaya which suggest that debris-cover on glaciers is increasing (Bolch et al. 2008; Bhambri et al. 2011; Shukla et al. 2020). The analysis further revealed that the CGs numbering 54 recessed faster (5.11%) than the DCGs numbering 23 (1.79%) suggesting that the debris-cover significantly alters the thermal regime of the surface, which in turn influences the process of ablation beneath the debris layer (Table 3). The observed results are in line with the other studies conducted on assessing the impact of debris-cover on glacier melting in the Himalaya which have suggested that the debris-cover significantly impacts the glacier recession (Gardelle et al. 2013; Pratap et al. 2015; Ali et al. 2017; Debnath et al. 2019).

Surface Ice Velocity (SIV) estimates

The SIV of the 39 selected glaciers in the study area estimated during 1999/2000 and 2019/2020 periods are shown in Figure 4. The overall observed trend in the SIV of the glaciers resembles to the standard velocity pattern of the valley type glaciers where the glacier movement is generally low near the snout due to the minimal ice thickness and increases with the increasing elevation up to the transient snow line, where it reaches to its highest value due to the highest gradient and basal sliding due to the pressure of the melting ice (Wu et al. 2020; Singh et al. 2021). The minimum, maximum and average SIV of the

individual glacier are summarized in Table S2. The average SIV of all the 39 glaciers varies between 21.35 ±3.3 m a^{-1} during 1999/2000 and 16.68 ±1.9 m a^{-1} during 2019/2020. Analysis of the SIV (Table S2) indicates a substantial decrease in the SIV during the period from 2000-2020. However, the SIV rates show significant variation among the glaciers. The highest SIV is shown by G13 glacier (46.41 m a^{-1}) and the slowest by G36 glacier (8.0 m a^{-1}) during 2000 and 2020. The highest decrease in the SIV during the observation is noticed for the G34 glacier (31.57%) and the lowest for the G48 glacier (1.26%) (Table S2). Between 1999/2000 and 2019/2020, the SIV of all the glaciers decreased on an average by 23.27 % (1.16% a^{-1}) with the annual average ice velocity decrease of 0.23 m a^{-1}. The displacement observed over the non-glaciated terrain is considered as an uncertainty in SIV estimation which ranges from 1.9 to 3.3 m (Table S3) in our case and is in good agreement with the already published studies (Scherler et al. 2011; Garg et al. 2017; Bhushan et al. 2017; Shukla and Garg 2020).

Decreasing trend in the glacier velocity in the study area is in line with the various other studies reported in the other basins of the Himalaya. A recent study by Shukla and Garg 2020, based on 18 glaciers in the central Himalaya, reported an average SIV of 22.63 ±5.8 m a^{-1} in 1993-94, which decreased to 17.32 ±3.1 m a^{-1} in 2000-01 and further declined to 11.50 ±1.7 m a^{-1} in 2015-16. Bhattacharya et al. (2016) reported the SIV of ~46 ±7.5 m a^{-1} during 1993-94, ~50 ±7.2 m a^{-1} in 1998-99 and 43 ±5.1 m a^{-1} during 2013-14 for the Chorabari glacier in the central Himalaya. Similarly, Bhushan et al. (2018) reported average SIV of 42.42 ±5.6 m a^{-1} for glaciers in the Zanskar Himalaya during 1999-2000 which decreased to 35.44 ±5.6 m a^{-1} by 2013-14. The main reason for the reduction in the glacier velocity is the retreat, thinning and mass loss of glaciers and the consequent decrease in the glacier gradient and basal sliding (Bhushan et al. 2017). All these studies suggested that the variations in SIV reflect the changes in evolution of ice flux in the middle and upper parts of the glaciers, consequently causing the dynamic feedbacks in the mass budgeting of a glacier.

Glacier mass changes

Accurate assessment of glacier mass loss is essential for understanding the glacier sensitivity to climate change. Thickness change showed a spatial variation across the studied glaciers in the study area. The thinning and thickening suggest that the glaciers are losing mass. Specific mass balance (SMB) rate of the selected glaciers was obtained using the bias-corrected DEMs and the same are shown in Table S4. It was observed that the SMB rate of different glaciers varied from -1.55 ±0.37 to -0.36 ±0.33 m w.e.a^{-1}. The most negative SMB rate is shown by G17 glacier (-1.55±0.37 m w.e.a^{-1}) while the G18 glacier experienced the lowest mass loss rate (-0.36±0.33 m w.e.a^{-1}) among the studied 77 glaciers in the region. The mean SMB rate of all the glaciers in the region is -1.08±0.31 m w.e.a^{-1} (Abdullah et al. 2020). The mass loss is often regarded as the most visible indicator of glaciers responding to climate change.

Vehicular pollution and black carbon concentration

Various studies on BC have reported that an increase in BC concentration in the atmosphere contributes significantly to the atmospheric warming as BC is highly heat absorbing atmospheric constituent, thus enhancing the glacier ablation (Ramanathan et al. 2007; Xu et al. 2009). From the black carbon observations in the study area, it was observed that BC concentration varied from 287 ng/m^3 to 3726 ng/m^3 with an average concentration of 1518 ng/m^3 (Figure 5) which is markedly higher compared to the BC concentration reported from the other high altitude locations in the Hindu Kush Himalaya (Table S5) (Zeb et al. 2020; Nair et al. 2013). Further, from the trend analysis of the time series of BC data from 1980-2020 (Figure 6), it was observed that the BC concentration has increased significantly with minimum value of ~338 ng/m^2 in 1984 rising to the maximum of ~634 ng/m^2 in 2020. It is thus inferred that the increasing BC concentration, due to the proximity to the national highway (NH), has significantly affected the glacier health as is evident from the glacier area shrinkage, snout retreat and mass loss of the glaciers observed in the study area. It was observed that the proximal glaciers, numbering 17, have showed higher glacier shrinkage (4.11%) and snout retreat (209m) compared to the distant glaciers, numbering 60, situated away from the NH which showed the glacier shrinkage of 2.82% and snout retreat of 148m during the observation period (Table 5).

Vehicular pollution

Transport sector forms the bulk of CO_2 and other greenhouse gas emissions from fossil fuel combustion. About 48% of the total freight plying on the national highway passing through the study area is composed of the heavy motor vehicles, which include buses, trucks, minibuses, heavy-duty trucks, sumo, jeeps and trailers, which run on diesel fuel. The remaining 52% of the traffic includes light motor transport like two wheelers, three wheelers, cars and others, which run on petrol fuel. The annual emission of CO_2, NOx, BC, CH4, and PM for different vehicle categories during 2011-2020 is shown in Figure 7, Table7. The annual emissions of the GHGs and particulate matter increased from 1728, 116, 22.34, 5.66, 0.64 and 1.28 tonnes in 2011 to 4413, 56.36, 13.20, 1.43 and 3.05 tonnes in 2020 for CO_2, NOx, BC, CH_4, and PM respectively indicating an annual growth rate of 11.8%, 11.07%, 11.4%, 11.4%, and 11.6% for CO_2, NOx, BC, CH_4, and PM respectively due to the increase in the traffic load. Overall, the emissions of CO_2, NOx, BC, CH_4, and PM have increased by around 39% during the study period. It is observed that the heavy motor vehicles are the major contributors of CO_2 emissions constituting 90% of the total CO_2 emission load. Light motor vehicles, which run on petrol or gasoline fuel, contributed about 56% of the total CH_4 emission load primarily due to their large number plying on the NH. For NO_X emission, the heavy motor vehicles contribute 88% of the total NO_X emission load. Buses, goods carrying vehicles and others are the major contributors of PM emissions contributing 79% of the particulate matter pollution. Heavy motor vehicles contribute 60% of BC emissions. The maximum emission of GHGs and particulate pollution was observed during year 2019 in which the total emission load from all the vehicle categories was about 5274, 68, 17, 2.0 and 4.0 tonnes/year of CO_2, NOx, BC, CH_4, and PM respectively.

The increasing emissions of the GHGs contribute to the global warming effect which enhances the melting of glaciers in the region. On the other hand, heating by black carbon warms the atmosphere at

elevated levels from 2 to 6 km (Ramanathan and Feng 2009), where most of the glaciers are located in the study area, thus strengthening the effect of GHGs on retreat of snow packs and glaciers in the region

Greenhouse gas data analysis

The major GHG's are CO_2, which causes 9-26% of the greenhouse effect on earth, water vapour causing about 36-70%, O_3 causing 3-7% and CH_4 contributing 4-9% (Griggs and Noguer 2002). In this study, the average monthly values of the GHGs were used to know the GHGs trends over the study area (Table 7). Figure 10 shows the monthly distribution of AIRS, GOSAT, and OMI GHGs data. The maximum CH_4 was found during the months of August, September and October (Table S6). The overall time series shows an increasing trend with 18.3 ppb $year^{-1}$ with the CH_4 values ranging between 1812-1944 ppb with the maximum concentration of the GHG during spring and summer months (Figure 10-I). The increasing trend in CH_4 is primarily attributed to the global increase emissions from the natural and anthropogenic sources, however the semi-arid climate of the study area with almost no vegetation grows compounds the problem (Kavitha et al. 2018).

The maximum O_3 concentration is found during the months of April, May and June (Table 7, S5). The overall time series shows an increasing trend with 0.25 ppb $year^{-1}$ with the values ranging between 43 and 69 ppb (Figure 10-II). Because of the cold desert nature of the study region characterized with cold semi-arid climate, where negligible vegetation cover (Juyal 2014), CO_2 sequestration is almost absent in the region.

The monthly daytime/night-time retrievals of water vapour distribution is shown in Figure 10-III and the total columnar water vapour values range between 7–47 kg/m^2. No trend is observed from the time series analysis of water vapour data. However, the monthly mean values show a distinct seasonal variation, with the maximum during summer season (average of 39kg/m^2) and minimum during the winter season (average of 10.5 kg/m^2) (Table S6).

CO_2 monthly mean values of total load over the study calculated from GOSAT measurements are plotted in the Figure 10-IV from January 2009 to December 2019. Almost every year, the CO_2 maxima is observed in March, April, May and June and the minima in August and September (Table S6). The CO_2 values range between 379-413 ppm with maximum during winters and minimum during autumn (Table 7, S5). The overall time series shows an increasing trend (1.5 ppm $year^{-1}$). CO_2 emission, transport sector and military operations may cause an increase in the local CO_2 levels (Al-Bayati and Al-Salihi 2019)

Figure 10-V shows the monthly variation of NO_2 in the tropospheric column over the study with an increasing trend observed during 2005-2015 period. An annual increase of 0.72% is observed in NO_2 which is $1.2*10^{13}$ molecules cm^2 year-^{1}. The average NO_2 value over the analysis is $1.3*10^{15}$ molecules cm^2. The highest concentration is observed during the summer months of May and June and the lowest during February (Table 7). Several factors contribute to the observed seasonal changes and the

increasing trend of the GHG (Lamsal et al. 2014) but the close proximity to the national highway and the heavy traffic in the area is one of the important factors contributing to the higher values of the NO_2 over the study area.

Climate data analysis

The trend analysis of the mean annual temperature data from 1901-2019 is shown in Figure 8. Based on the Mann-Kendall test, the analysis the mean annual temperature showed statistically significant continuous increasing trend from 1901-2019 at <0.01 and the Z statistic value > 2.57, which indicates the high significance of the observed trend. It was further, observed that the mean annual temperature of the 1901-1940 period (1.13°C) was lower than that observed during 1941-1980 period (1.43°C). The mean annual temperature further increased significantly during 1981-2019 to 1.69°C suggesting that there is a significant increase in the mean temperature in the region during the last few decades. This significant increase in the mean temperature in the region, due to the increasing GHGs, PM, and BC might be one of the possible reasons for the glacier recession observed in the study area. Various studies have shown that there is a strong negative correlation between glacier recession and temperature (Zhang et al 2014; Mandal et al. 2016).

Similarly, CRU based precipitation data analysis showed the average precipitation of 635 mm was recorded during 1901-2019 (Figure 9). The Precipitation trend analysis suggests that there is inter-annual variability in the overall precipitation with decreasing but non-significant trend during 1901-1940, increasing but non-significant trend during 1941-1980 and almost flat average precipitation during 1981-2019 indicating that the precipitation over the region has remained almost constant during the last few decades which coincides with the observed glacier recession during the last few decades. This suggests that the region has experienced a warmer climate during the past several decades which, under the no-change precipitation scenario, might be the reason for the observed glacier recession in the Himalayan region.

Conclusion

Bidecadal basin-wide assessment of the host of glacier parameters viz., glacier shrinkage, snout retreat, glacier thickness change, mass loss and glacier velocity and its strong correspondence with the increasing concentration of the GHGs, BC and other pollutants due to the anthropogenic activities, the consequent climate change mainly drives the glacier melting in the basin which showed the average glacier mass loss of -1.08±0.31 m w.e.a^{-1}.

In light of the differential response of the glaciers to climate change in the Himalaya, and the fact that the observation of climate, CHGs and other pollutants are far and few in the inaccessible regions, the use of frequent, synoptic and high-resolution remotely sensed observations of the glacier parameters, GHGs, pollutants and other driving factors provided a reliable alternative. The local emissions of black carbon and other short-lived pollutants from the burning of fossil fuels and woody biomass compounds the

impacts of climate change on the melting of glacier and needs to be accounted for when assessing the impact of climate change on glacier melting. Given the limited observations of BC and other pollutants in the basin, it is important to strengthen the observation network in the data-scarce Himalaya to improve our understanding of the impacts of local anthropogenic drivers and global climate change on cryospheric melting in order to fill the knowledge gaps.

It is a worry that, if, the observed trends of the climate change continue in the future due to the enhanced emissions of greenhouse gasses, and anthropogenic pollution, the glaciers might disappear altogether in the Himalaya leading to the significant impact on the regional water supplies, hydrological processes, ecosystem services and transboundary sharing of waters.

Declarations

Statements and Declarations

Author Contributions

Shakil Ahmad Romshoo: Conceptualization, Methodology, Investigation, Supervision, Writing and Preparation of the manuscript; Khalid Omar Murtaza: Data curation and Analysis, Methodology, Investigation, Manuscript preparation, writing, review; Waheed Shah: Data curation and Analysis; Tawseef Ramzan: Data analysis and Investigation; Ummer Ameen: Data analysis and editing and Mustafa Hameed Bhat: Data analysis and Editing.

Funding

The work was conducted as part of the research grant received from the Department of Science and Technology (DST), Government of India under the research project titled “Centre of Excellence for Glacial Studies in Western Himalaya”.

Competing Interests

The authors declare that they have no known competing financial interests or personal relationships that could have appeared to influence the work reported in this paper.

Ethics approval and consent to participate

Not applicable.

Consent for publication

Not applicable.

Data availability and materials

The datasets used during the current study are available from the corresponding author on reasonable request.

References

Abdullah T, Romshoo SA, Rashid I (2020) The satellite observed glacier mass changes over the Upper Indus Basin during 2000–2012. Scientific reports 10:1-9.

Al-Bayati RM, Al-Salihi AM (2019) Monitoring carbon dioxide from (AIRS) over Iraq during 2003-2016. In AIP Conference Proceedings. 2144(1):030007. AIP Publishing LLC.

Ali I, Shukla A, Romshoo SA (2017) Assessing linkages between spatial facies changes and dimensional variations of glaciers in the upper Indus Basin, western Himalaya. Geomorphology 284:115-129.

Ali S, Khan G, Hassan W, Qureshi JA, Bano I (2021) Assessment of glacier status and its controlling parameters from 1990 to 2018 of Hunza Basin, Western Karakorum. Environmental Science and Pollution Research 1-13.

Arendt AA, Echelmeyer KA, Harrison WD, Lingle CS, Valentine VB (2002) Rapid wastage of Alaska glaciers and their contribution to rising sea level. Science 297:382-386.

Ayoub F, Leprince S, Keene L (2009) User's guide to COSI-CORR co-registration of optically sensed images and correlation. California Institute of Technology: Pasadena, CA, USA, 38.

Baidya S, Borken-Kleefeld J (2009) Atmospheric emissions from road transportation in India. Energy Policy 37:3812-3822.

Bajracharya SR, Maharjan SB, Shrestha F (2014) The status and decadal change of glaciers in Bhutan from the 1980s to 2010 based on satellite data. Annals of Glaciology 55:159-166.

Barry R, Gan TY (2011) The global cryosphere: past, present and future. Cambridge University Press.

Bhambri R, Bolch T, Chaujar RK, Kulshreshtha SC (2011) Glacier changes in the Garhwal Himalaya, India, from 1968 to 2006 based on remote sensing. Journal of Glaciology 57:543-556.

Bhat MA, Romshoo SA, Beig G (2017) Aerosol black carbon at an urban site-Srinagar, Northwestern Himalaya, India: Seasonality, sources, meteorology and radiative forcing. Atmospheric Environment 165:336-348.

Bhattacharya A, Bolch T, Mukherjee K, Pieczonka T, Kropáček JAN, Buchroithner MF (2016) Overall recession and mass budget of Gangotri Glacier, Garhwal Himalayas, from 1965 to 2015 using remote sensing data. Journal of Glaciology 62:1115-1133.

Bhushan S, Syed TH, Arendt AA, Kulkarni AV, Sinha D (2018) Assessing controls on mass budget and surface velocity variations of glaciers in Western Himalaya. Scientific reports 8:1-11.

Bhushan S, Syed TH, Kulkarni AV, Gantayat P, Agarwal V (2017) Quantifying changes in the Gangotri Glacier of Central Himalaya: Evidence for increasing mass loss and decreasing velocity. IEEE Journal of Selected Topics in Applied Earth Observations and Remote Sensing 10:5295-5306.

Bolch T, Buchroithner MF, Peters J, Baessler M, Bajracharya S (2008) Identification of glacier motion and potentially dangerous glacial lakes in the Mt. Everest region/Nepal using spaceborne imagery. Natural Hazards and Earth System Sciences. 8, 1329-1340.

Bolch T, Kulkarni A, Kääb A, Huggel C, Paul F, Cogley JG et al (2012) The state and fate of Himalayan glaciers. Science 336:310-314.

Bolch T, Menounos B, Wheate R (2010) Landsat-based inventory of glaciers in western Canada, 1985–2005. Remote sensing of Environment 1141:127-137.

Chahine MT, Pagano TS, Aumann HH, Atlas R, Barnet C, Blaisdell J et al (2006) AIRS: Improving weather forecasting and providing new data on greenhouse gases. Bulletin of the American Meteorological Society 87:911-926.

Chand P, Sharma MC (2015) Glacier changes in the Ravi basin, North-Western Himalaya (India) during the last four decades (1971–2010/13). Global and Planetary Change 135:133-147.

Chudley TR, Miles ES, Willis IC (2017) Glacier characteristics and retreat between 1991 and 2014 in the Ladakh Range, Jammu and Kashmir. Remote Sensing Letters 8:518-527.

Cogley JG (2011) Present and future states of Himalaya and Karakoram glaciers. Annals of Glaciology 52:69-73.

Das S, Sharma MC (2019) Glacier changes between 1971 and 2016 in the Jankar Chhu Watershed, Lahaul Himalaya, India. Journal of Glaciology 65:13-28.

DeBeer CM, Sharp MJ (2009) Topographic influences on recent changes of very small glaciers in the Monashee Mountains, British Columbia, Canada. Journal of Glaciology 55:691-700.

Debella-Gilo M, Kääb A (2011) Sub-pixel precision image matching for measuring surface displacements on mass movements using normalized cross-correlation. Remote Sensing of Environment 115:130-142.

Debnath M, Sharma MC, Syiemlieh HJ (2019) Glacier dynamics in changme khangpu basin, Sikkim Himalaya, India, between 1975 and 2016. Geosciences 9:259.

Dehecq A, Gourmelen N, Gardner AS, Brun F, Goldberg D, Nienow PW et al (2019) Twenty-first century glacier slowdown driven by mass loss in High Mountain Asia. Nature Geoscience 12:22-27.

Ding C, Feng G, Li Z, Shan X, Du Y, Wang H (2016) Spatio-temporal error sources analysis and accuracy improvement in Landsat 8 image ground displacement measurements. Remote Sensing 8:937.

Diolaiuti GA, Bocchiola D, Vagliasindi M, D'agata C, Smiraglia C (2012) The 1975–2005 glacier changes in Aosta Valley (Italy) and the relations with climate evolution. Progress in Physical Geography 36:764-785.

Dixit A, Sahany S, Kulkarni AV (2021) Glacial changes over the Himalayan Beas basin under global warming. Journal of Environmental Management 295:113101.

Dobhal DP, Mehta M, Srivastava D (2013) Influence of debris cover on terminus retreat and mass changes of Chorabari Glacier, Garhwal region, central Himalaya, India. Journal of Glaciology 59:961-971.

Farinotti D, Immerzeel WW, de Kok RJ, Quincey DJ, Dehecq A (2020) Manifestations and mechanisms of the Karakoram glacier Anomaly. Nature Geoscience 13:8-16.

Fujita K, Nuimura T (2011) Spatially heterogeneous wastage of Himalayan glaciers. Proceedings of the National Academy of Sciences 108:14011-14014.

Gao J, Liu Y (2001) Applications of remote sensing, GIS and GPS in glaciology: a review. Progress in Physical Geography 25:520-540.

Gardelle J, Berthier E, Arnaud Y, Kääb A (2013) Region-wide glacier mass balances over the Pamir-Karakoram-Himalaya during 1999–2011. The Cryosphere 7:1263-1286.

Garg PK, Shukla A, Tiwari RK, Jasrotia AS (2017) Assessing the status of glaciers in part of the Chandra basin, Himachal Himalaya: a multiparametric approach. Geomorphology 284:99-114.

Granshaw FD, Fountain AG (2006) Glacier change (1958–1998) in the north Cascades national park complex, Washington, USA. Journal of Glaciology 52:251-256.

Griggs DJ, Noguer M (2002) Climate change 2001: the scientific basis. Contribution of working group I to the third assessment report of the intergovernmental panel on climate change. Weather 57:267-269.

Hall DK, Bayr KJ, Schöner W, Bindschadler RA Chien JY (2003) Consideration of the errors inherent in mapping historical glacier positions in Austria from the ground and space (1893–2001). Remote Sensing of Environment 86:566-577.

Harris I, Osborn TJ, Jones P, Lister D (2020) Version 4 of the CRU TS monthly high-resolution gridded multivariate climate dataset. Scientific data 7:1-18.

Heid T, Kääb A (2012) Evaluation of existing image matching methods for deriving glacier surface displacements globally from optical satellite imagery. Remote Sensing of Environment 118:339-355.

Heid T (2011) Deriving glacier surface velocities from repeat optical images. Ph.D. Thesis. Department of Geosciences, Faculty of Mathematics and Natural Sciences, University of Oslo, Oslo.

Hewitt K (2005) The Karakoram anomaly? Glacier expansion and the 'elevation effect' Karakoram Himalaya. Mountain Research and Development 25:332-340.

Hoelzle M, Haeberli W, Dischl M, Peschke W (2003) Secular glacier mass balances derived from cumulative glacier length changes. Global and Planetary Change 36:295-306.

Huss M, Fischer M (2016) Sensitivity of very small glaciers in the Swiss Alps to future climate change. Frontiers in Earth Science 4:34.

Immerzeel WW, Van Beek LP, Bierkens MF (2010) Climate change will affect the Asian water towers. Science 328:1382-1385.

Jiskoot H, Curran CJ, Tessler DL, Shenton LR (2009) Changes in Clemenceau Icefield and Chaba Group glaciers, Canada, related to hypsometry, tributary detachment, length–slope and area–aspect relations. Annals of Glaciology 50:133-143.

Juyal N (2014) Ladakh: the high-altitude Indian cold desert. In Landscapes and Landforms of India. Springer, Dordrecht.

Kääb A (2002) Monitoring high-mountain terrain deformation from repeated air-and space borne optical data: examples using digital aerial imagery and ASTER data. ISPRS Journal of Photogrammetry and remote sensing 57:39-52.

Kääb A, Huggel C, Fischer L (2006) Remote sensing technologies for monitoring climate change impacts on glacier-and permafrost-related hazards.

Kääb A, Huggel C, Fischer L, Guex S, Paul F, Roer I et al (2005) Remote sensing of glacier-and permafrost-related hazards in high mountains: an overview. Natural Hazards and Earth System Sciences 5:527-554.

Kavitha M, Nair PR, Girach IA, Aneesh S, Sijikumar S, Renju R (2018) Diurnal and seasonal variations in surface methane at a tropical coastal station: Role of mesoscale meteorology. Science of the Total Environment 631:1472-1485.

Kendall K (1975) Thin-film peeling-the elastic term. Journal of Physics D: Applied Physics 8:1449.

Khan G, Ali S, Xiangke X, Qureshi JA, Ali M, Karim I (2021) Expansion of Shishper Glacier lake and recent glacier lake outburst flood (GLOF), Gilgit-Baltistan, Pakistan. Environmental Science and Pollution Research 28(16):20290-20298.

Koul MN, Bahuguna IM, Rajawat AS, Ali S, Koul S (2016) Glacier area change over past 50 years to stable phase in Drass valley, Ladakh Himalaya (India). American Journal of Climate Change 5:88.

Kramer RJ, He H, Soden BJ, Oreopoulos L, Myhre G, Forster PM, Smith CJ (2021) Observational evidence of increasing global radiative forcing. Geophysical Research Letters 48(7):e2020GL091585.

Krotkov NA, McLinden CA, Li C, Lamsal LN, Celarier EA, Marchenko SV et al (2016) Aura OMI observations of regional SO2 and NO2 pollution changes from 2005 to 2015. Atmospheric Chemistry and Physics 16:4605-4629.

Kumar D, Singh AK, Taloor AK, Singh DS (2021) Recessional pattern of Thelu and Swetvarn glaciers between 1968 and 2019, Bhagirathi basin, Garhwal Himalaya, India. Quaternary International 575:227-235.

Kuze A, Suto H, Nakajima M, Hamazaki T (2009) Thermal and near infrared sensor for carbon observation Fourier-transform spectrometer on the Greenhouse Gases Observing Satellite for greenhouse gases monitoring. Applied optics 48:6716-6733.

Lamsal LN, Krotkov NA, Celarier EA, Swartz WH, Pickering KE, Bucsela, EJ et al (2014) Evaluation of OMI operational standard NO 2 column retrievals using in situ and surface-based NO2 observations. Atmospheric Chemistry and Physics 14:11587-11609.

Lemke P, Ren J, Alley RB, Allison I, Carrasco J, Flato G et al (2007) Observations: changes in snow, ice and frozen ground.

Leprince S, Barbot S, Ayoub F, Avouac JP (2007) Automatic and precise orthorectification, coregistration, and subpixel correlation of satellite images, application to ground deformation measurements. IEEE Transactions on Geoscience and Remote Sensing 45:1529-1558.

Mandal A, Ramanathan AL, Angchuk T, Soheb M, Singh VB (2016) Unsteady state of glaciers (Chhota Shigri and Hamtah) and climate in Lahaul and Spiti region, western Himalayas: a review of recent mass loss. Environmental Earth Sciences 75:1-12.

Mann HB (1945) Nonparametric tests against trend. Econometrica: Journal of the econometric society 245-259.

Murtaza KO, Romshoo SA (2014) Determining the suitability and accuracy of various statistical algorithms for satellite data classification. International journal of geomatics and geosciences 4:585.

Murtaza KO, Romshoo SA (2017) Recent glacier changes in the Kashmir alpine Himalayas, India. Geocarto International 32:188-205.

Murtaza KO, Dar RA, Paul OJ, Bhat NA, Romshoo SA (2021) Glacial geomorphology and recent glacial recession of the Harmukh Range, NW Himalaya. Quaternary International 575:236-248.

Nainwal HC, Banerjee A, Shankar R, Semwal P, Sharma T (2016) Shrinkage of Satopanth and Bhagirath Kharak glaciers, India, from 1936 to 2013. Annals of glaciology 57:131-139.

Nair VS, Babu SS, Moorthy KK, Sharma AK, Marinoni A, Ajai (2013) Black carbon aerosols over the Himalayas: direct and surface albedo forcing. Tellus B: Chemical and Physical Meteorology 65:19738.

Nuth C, Kääb A (2011) Co-registration and bias corrections of satellite elevation data sets for quantifying glacier thickness change. The Cryosphere 5:271-290.

Oerlemans J, Fortuin JPF (1992) Sensitivity of glaciers and small ice caps to greenhouse warming. Science 258:115-117.

Pall IA, Meraj G, Romshoo SA (2019) Applying integrated remote sensing and field-based approach to map glacial landform features of the Machoi Glacier valley, NW Himalaya. SN Applied Sciences 1(5):1-11.

Pandey P, Venkataraman G (2013) Changes in the glaciers of Chandra–Bhaga basin, Himachal Himalaya, India, between 1980 and 2010 measured using remote sensing. International Journal of Remote Sensing 34:5584-5597.

Patel LK, Sharma P, Fathima TN, Thamban M (2018) Geospatial observations of topographical control over the glacier retreat, Miyar basin, Western Himalaya, India. Environmental earth sciences 77:1-12.

Paul F (2015) Revealing glacier flow and surge dynamics from animated satellite image sequences: examples from the Karakoram. The Cryosphere 9:2201-2214.

Paul F, Bolch T, Briggs K, Kääb A, McMillan M, McNabb R (2017) Error sources and guidelines for quality assessment of glacier area, elevation change, and velocity products derived from satellite data in the Glaciers_cci project. Remote Sensing of Environment 203:256-275.

Paul F, Kääb A, Maisch M, Kellenberger T, Haeberli W (2002) The new remote-sensing-derived Swiss glacier inventory: I. Methods. Annals of Glaciology 34:355-361.

Prakash J, Habib G (2018) A technology-based mass emission factors of gases and aerosol precursor and spatial distribution of emissions from on-road transport sector in India. Atmospheric Environment 180:192-205.

Pratap B, Dobhal DP, Mehta M, Bhambri R (2015) Influence of debris cover and altitude on glacier surface melting: a case study on Dokriani Glacier, central Himalaya, India. Annals of Glaciology 56:9-16.

Racoviteanu AE, Arnaud Y, Williams MW, Ordonez J (2008) Decadal changes in glacier parameters in the Cordillera Blanca, Peru, derived from remote sensing. Journal of Glaciology 54:499-510.

Ramachandra TV, Aithal BH, Sreejith K (2015) GHG footprint of major cities in India. Renewable and Sustainable Energy Reviews 44:473-495.

Ramanathan V, Feng Y (2009) Air pollution, greenhouse gases and climate change: Global and regional perspectives. Atmospheric Environment 43:37-50.

Ramanathan V, Ramana MV, Roberts G, Kim D, Corrigan C, Chung C, Winker D (2007) Warming trends in Asia amplified by brown cloud solar absorption. Nature 448:575-578.

Rashid I, Majeed U, Najar NA, Bhat IA (2021) Retreat of Machoi Glacier, Kashmir Himalaya between 1972 and 2019 using remote sensing methods and field observations. Science of the Total Environment 785:147376.

Ren J, Jing Z, Pu J, Qin X (2006) Glacier variations and climate change in the central Himalaya over the past few decades. Annals of Glaciology 43:218-222.

Richardson S (1999) Joint EMEP/CORINAIR Atmospheric emission inventory guidebook.

Romshoo SA, Fayaz M, Meraj G, Bahuguna IM (2020) Satellite-observed glacier recession in the Kashmir Himalaya, India, from 1980 to 2018. Environmental Monitoring and Assessment 192:1-17.

Sahu R, Gupta RD (2019) Spatiotemporal variation in surface velocity in Chandra basin glacier between 1999 and 2017 using Landsat-7 and Landsat-8 imagery. Geocarto International 1-21.

Sakai A, Fujita K (2017) Contrasting glacier responses to recent climate change in high-mountain Asia. Scientific reports 7:1-8.

Sam L, Bhardwaj A, Kumar R, Buchroithner MF, Martín-Torres FJ (2018) Heterogeneity in topographic control on velocities of Western Himalayan glaciers. Scientific reports 8:1-16.

Scherler D, Strecker MR (2012) Large surface velocity fluctuations of Biafo Glacier, central Karakoram, at high spatial and temporal resolution from optical satellite images. Journal of Glaciology 58:569-580.

Scherler D, Bookhagen B, Strecker MR (2011) Spatially variable response of Himalayan glaciers to climate change affected by debris cover. Nature Geoscience 4:156-159.

Scherler D, Leprince S, Strecker MR (2008) Glacier-surface velocities in alpine terrain from optical satellite imagery—Accuracy improvement and quality assessment. Remote Sensing of Environment 112:3806-3819.

Schmidt S, Nüsser M (2012) Changes of high altitude glaciers from 1969 to 2010 in the Trans-Himalayan Kang Yatze Massif, Ladakh, northwest India. Arctic, Antarctic, and Alpine Research 44:107-121.

Shrestha AB, Aryal R (2011) Climate change in Nepal and its impact on Himalayan glaciers. Regional environmental change 11:65-77.

Shukla A, Garg PK (2020) Spatio-temporal trends in the surface ice velocities of the central Himalayan glaciers, India. Global and Planetary Change 190:103187.

Shukla A, Garg S, Mehta M, Kumar V, Shukla UK (2020) Temporal inventory of glaciers in the Suru sub-basin, western Himalaya: impacts of regional climate variability. Earth System Science Data 12:1245-

1265.

Singh DK, Thakur PK, Naithani BP, Dhote PR (2021) Spatio-temporal analysis of glacier surface velocity in Dhauliganga basin using geo-spatial techniques. Environmental Earth Sciences 80:1-16.

Snehmani, Bhardwaj A, Pandit A, Ganju A (2014) Demarcation of potential avalanche sites using remote sensing and ground observations: a case study of Gangotri glacier. Geocarto International 29:520-535.

Storey JC, Choate MJ (2004) Landsat-5 bumper-mode geometric correction. IEEE Transactions on Geoscience and Remote Sensing 42:2695-2703.

Susskind J, Barnet CD, Blaisdell JM (2003) Retrieval of atmospheric and surface parameters from AIRS/AMSU/HSB data in the presence of clouds. IEEE Transactions on Geoscience and Remote Sensing 41:390-409.

Thakur VC, Rawat BS (1992) Geological map of the Western Himalaya. Published under the authority of the Surveyor General of India. Printing Group of Survey of India. 101.

Thompson I, Shrestha M, Chhetri N, Agusdinata DB (2020) An institutional analysis of glacial floods and disaster risk management in the Nepal Himalaya. International Journal of Disaster Risk Reduction 47:101567.

Tiwari RK, Gupta RP, Arora MK (2014) Estimation of surface ice velocity of Chhota-Shigri glacier using sub-pixel ASTER image correlation. Current Science 853-859.

Veh G, Korup O, von Specht S, Roessner S, Walz A (2019) Unchanged frequency of moraine-dammed glacial lake outburst floods in the Himalaya. Nature Climate Change 9:379-383.

Venkatesh TN, Kulkarni AV, Srinivasan J (2012) Relative effect of slope and equilibrium line altitude on the retreat of Himalayan glaciers. The cryosphere 6:301-311.

Vijay S, Braun M (2016) Elevation change rates of glaciers in the Lahaul-Spiti (Western Himalaya, India) during 2000–2012 and 2012–2013. Remote Sensing 8:1038.

Wu K, Liu S, Xu J, Zhu Y, Liu Q, Jiang Z, Wei J (2020) Spatiotemporal variability of surface velocities of monsoon temperate glaciers in the Kangri Karpo Mountains, southeastern Tibetan Plateau. Journal of Glaciology 1-6.

Xu B, Cao J, Hansen J, Yao T, Joswia DR, Wang N et al (2009) Black soot and the survival of Tibetan glaciers. Proceedings of the National Academy of Sciences 106:22114-22118.

Zeb B, Alam K, Nasir J, Mansha M, Ahmad I, Bibi S et al (2020) Black Carbon aerosol characteristics and radiative forcing over the high altitude glacier region of Himalaya-Karakorum-Hindukush. Atmospheric Environment 238:117711.

Zemp M, Frey H, Gärtner-Roer I, Nussbaumer SU, Hoelzle M, Paul F et al (2015) Historically unprecedented global glacier decline in the early 21st century. Journal of Glaciology 61:745-762.

Zhang G, Li Z, Wang W, Wang W (2014) Rapid decrease of observed mass balance in the Urumqi Glacier No. 1, Tianshan Mountains, central Asia. Quaternary International 349:135-141.

Zhao X, Wang X, Wei J, Jiang Z, Zhang Y, Liu S (2020) Spatiotemporal variability of glacier changes and their controlling factors in the Kanchenjunga region, Himalaya based on multi-source remote sensing data from 1975 to 2015. Science of the Total Environment 745:140995.

Tables

Table 1: Details of the data used in the study.

Datasets	Acquisition Date	Spatial Resolution (m)	Purpose/Use
Landsat-ETM+	19-08-1999/ 30-09-2000	15 (Pan) 30 (MS)	SIV/Mapping
Landsat-OLI	16-08-2019/ 05-10-2020	15 (Pan) 30 (MS)	SIV/Mapping
Google Earth Imagery		2.5/ 5	Validation
Shuttle Radar Topography Mission (SRTM)	2000	30/90 m	Topographical parameters (Slope, Aspect, Elevation)
TanDEM-X	2011-2015	90	Elevation
Atmospheric Infra-Red Sounder (AIRS)	2003-2020	1 degree	O_3, Water Vapor, and CH_4 Concentration
Greenhouse gases Observing Satellite (GOSAT)	2009-2019	1 degree	CO_2 Concentration
Ozone Monitoring Instrument (OMI)	2005-2020	0.25 degree	NO_2 Concentration

Table 2: Comparison of the various glacier recession studies conducted in the neighbourhood of the study area.

Authors	Region	No. of Glaciers	Study Period	Area Change (%)	Recession rate ($\% yr^{-1}$)
Koul et al. (2016)	Drass	81	1965-2013	-16.63	0.34
Chudley et al. (2017)	Ladakh	657	1991-2014	-12.8	0.55
Shukla et al. (2020)	Suru	252	1971-2017	-6.02	0.13
Romshoo et al. (2020)	Kashmir	147	1980-2018	-28.82	0.75
Rashid et al. (2021)	Drass	1	1972-2019	-29.00	0.62
*Current Study	Drass	77	2000-2020	-3.00	0.14

Table 3: Influences of the glacier size and debris-cover on glacier recession in the study area.

Category	Number	Area km^2		Area Change (km^2)	% Change
		2000	2020		
Glacier Size					
<1	29	17.4±1.66	16.01±1.58	1.39±0.08	7.99
1-5	40	96.41±6.21	93.45±6.01	2.94±0.20	4.11
>5	8	62.96±2.83	62±2.78	0.96±0.05	2.22
Total	**77**	**176.77±10.70**	**171.46±10.37**	**5.31±0.33**	**3.00**
Debris-covered glaciers					
Debris-covered (DCGs)	23	106.72±4.87	104.81±4.75	1.91±0.12	1.79
Non-Debris- covered (CGs)	54	70.05±5.84	66.65±5.61	3.58±0.23	5.11

Table 4: Influence of elevation and slope on glacier recession in the study area

Category	Number	Area (km^2)		Area Change	
		2000	2020	(Km^2)	% Change
Elevation					
4600-5000	31	41.71±2.40	40±2.28	1.71±0.12	4.10
5000-5400	38	91±5.47	88.06±5.30	2.94±0.17	3.23
5400-5800	8	44.06±2.83	43.40±2.78	0.64±0.05	1.46
Slope					
<15	21	83.46±3.71	81.52±3.61	1.94±0.10	2.32
>15	56	93.31±7.00	89.92±6.75	3.35±0.25	3.59

Table 5: Influence of national highway proximity and the consequent vehicular pollution on the glacier recession in the study area.

National Highway Proximity	Number	Area (km^2)		Area Change	Snout retreat	Elevation change (dh/dt)
		2000	2020	(%)	(m)	($m\ yr^{-1}$)
Proximal glaciers	17	37.44	35.90	4.11	209	-1.37
Distant glaciers	60	139.27	135.33	2.82	148	-1.24

Table 6: Emission of GHGs, BC and PM from vehicular pollution during 2011-2020 in the study area

Year	CO_2	NOx	BC	CH_4	PM
	(tonnes/year)				
2011	1728.08	22.34	5.66	0.64	1.28
2012	2456.23	31.37	7.37	0.80	1.70
2013	3234.02	41.36	9.80	1.07	2.26
2014	3277.99	42.04	10.14	1.12	2.33
2015	3488.78	44.71	10.74	1.18	2.47
2016	4275.28	54.98	13.49	1.50	3.08
2017	4559.81	58.80	14.68	1.65	3.33
2018	5022.27	64.83	16.29	1.84	3.69
2019	5274.42	67.97	16.90	1.90	3.84
2020	4413.91	56.36	13.20	1.43	3.05
References	(Baidya et al., 2009)	(Richardson, 1999)	(Prakash et al., 2018)	(Richardson, 1999)	(Baidya et al., 2009)

Table 7: Statistical analysis of the GHGs over the study area.

Parameter	Max.	Min.	Mean	Trend $year^{-1}$	Significance
O_3 ppb (AIRS)	73	44	56	+0.25	0.001
Water vapour kg/m^2 (AIRS)	47	9.2	22	0	
CH_4 (AIRS)	1994	1812	1870	+18.3	0.001
NO_2 molecules cm^2 (OMI)	2.6E+15	1.5E+14	1.3E+15	+1.2E9	0.001
CO_2 ppm (GOSAT)	413	379	396	+1.5	0.001

Figures

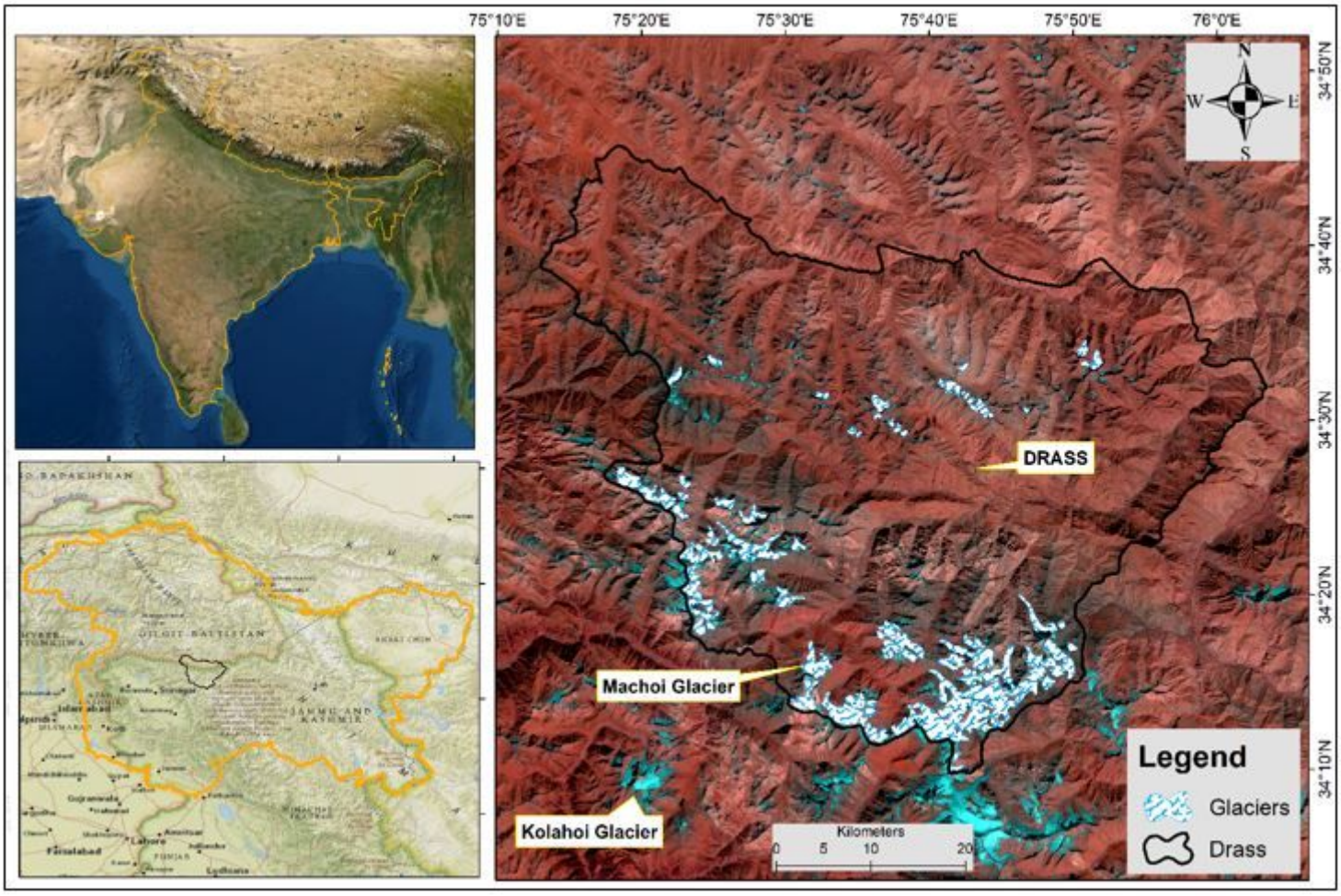

Figure 1

Location and distribution of glaciers in the Drass region, western Himalaya, India

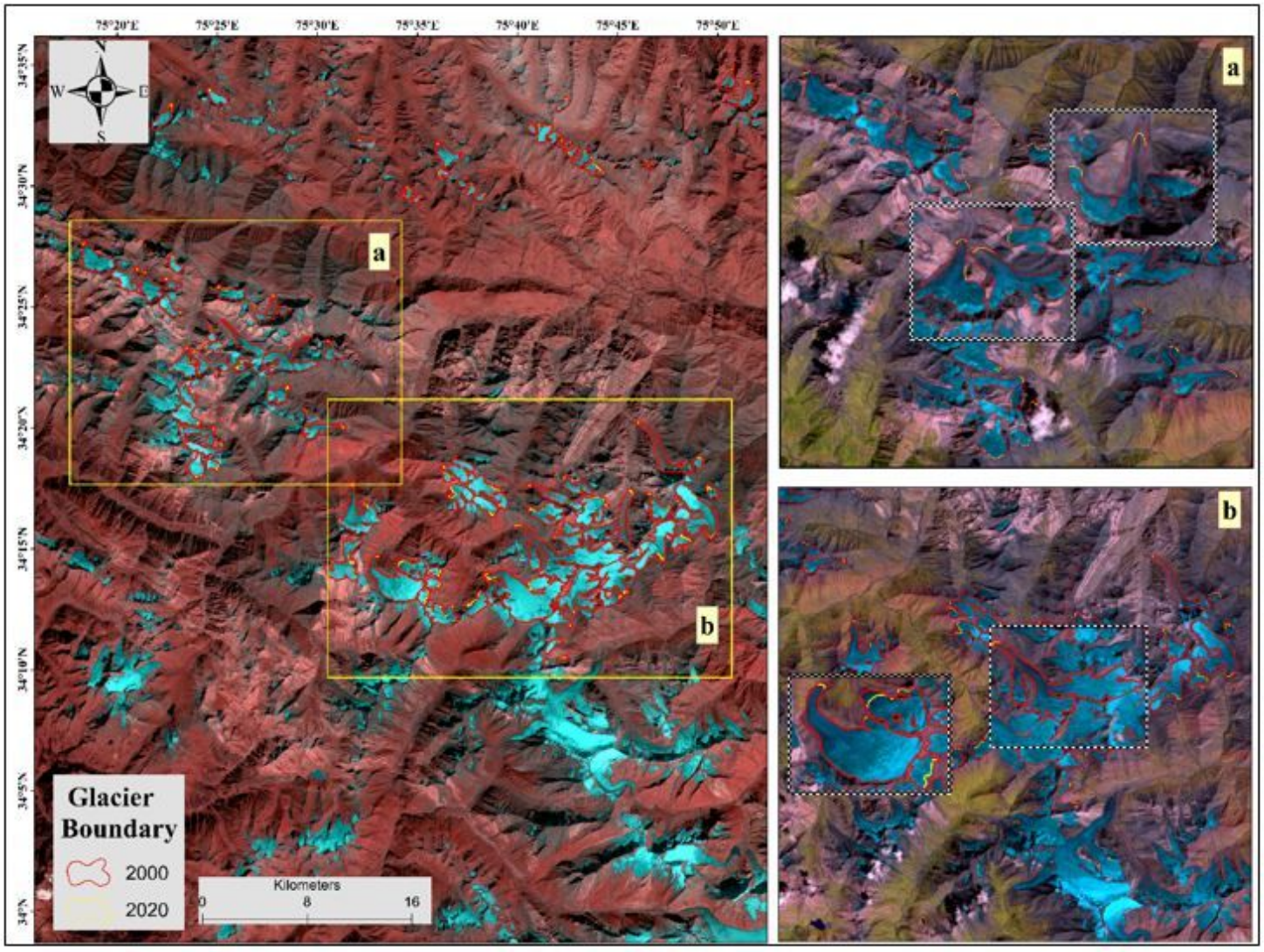

Figure 2

Zoomed-in view of the glacier recession from 2000 to 2020 in the study area

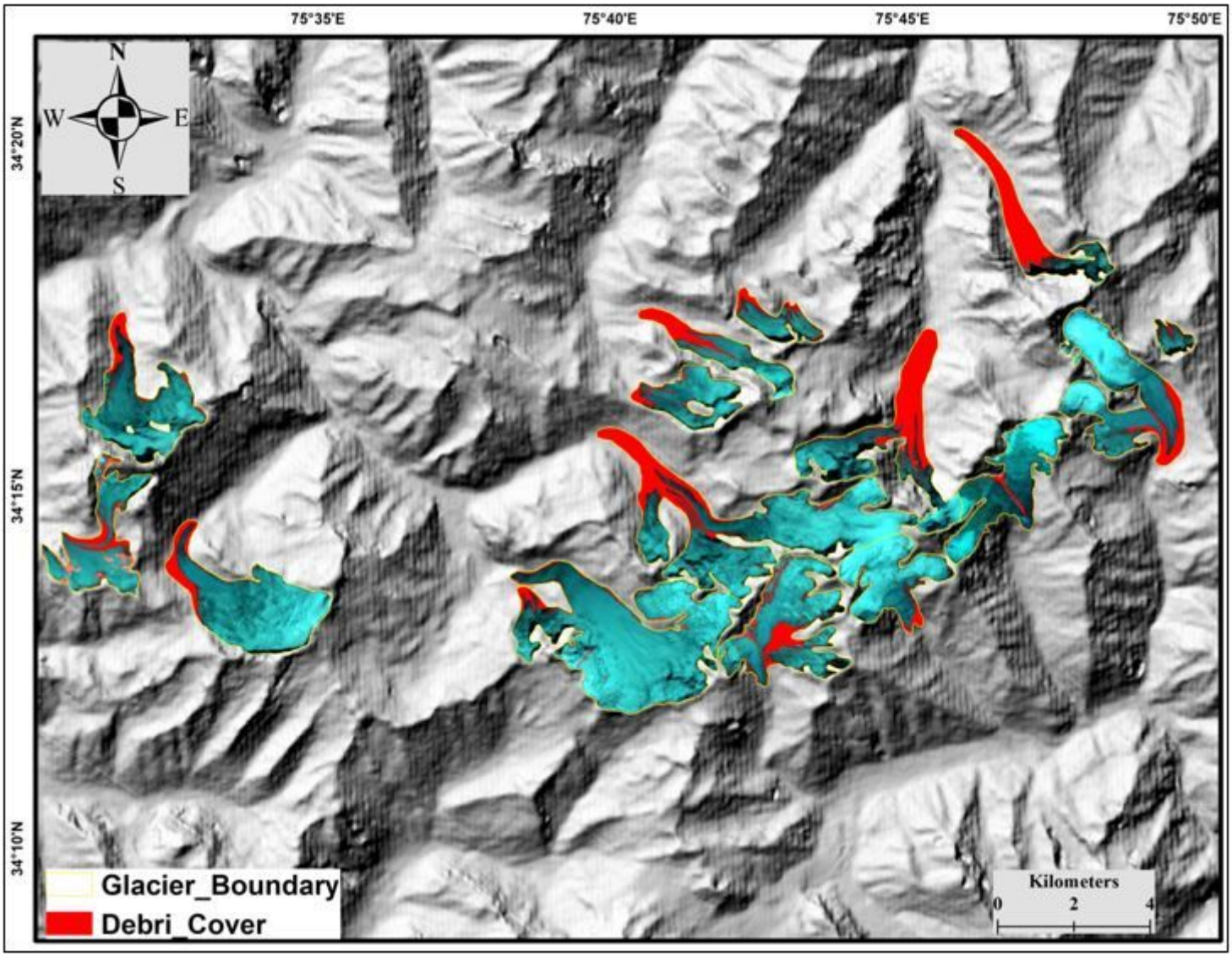

Figure 3

Some of the debris-covered glaciers in the study area

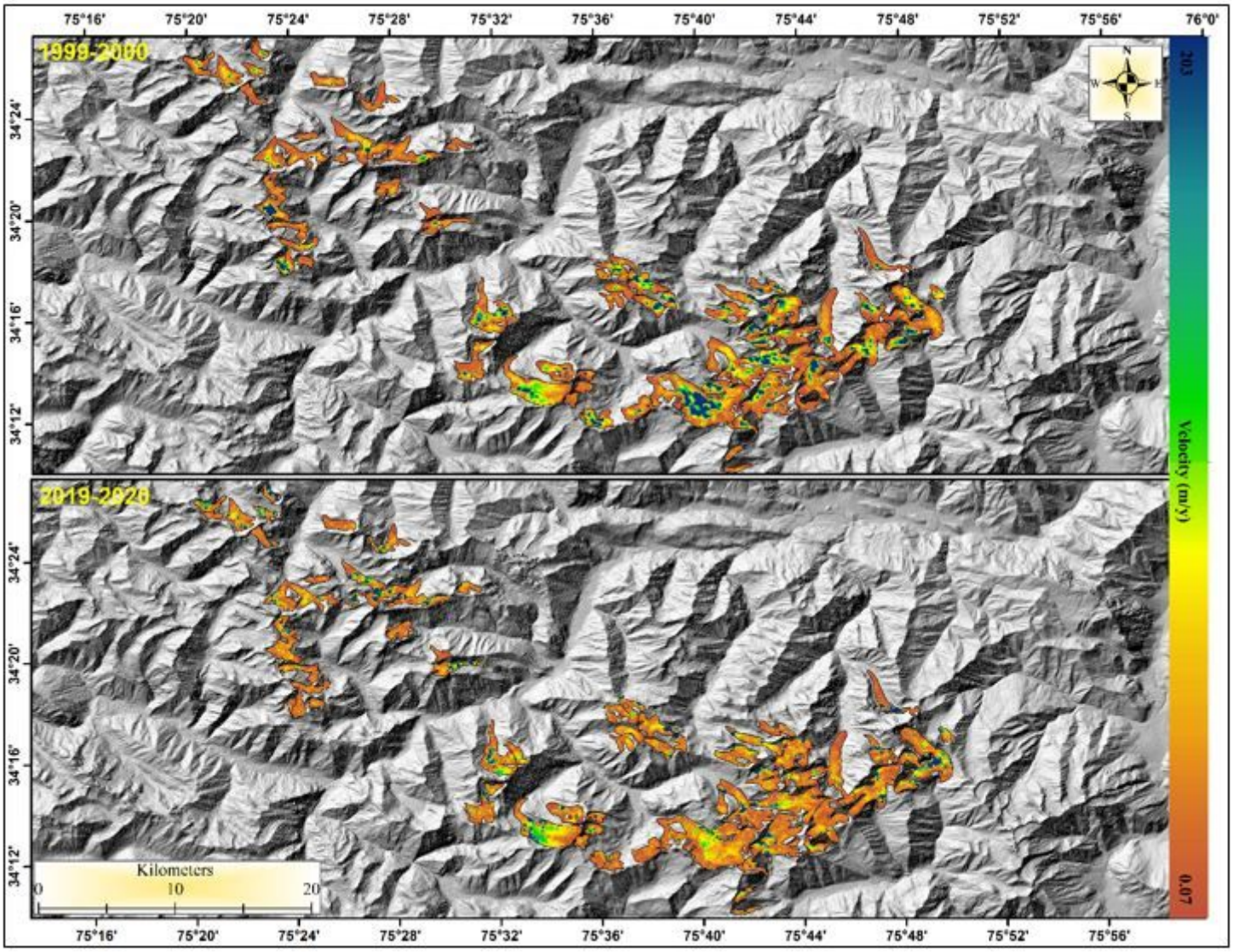

Figure 4

Surface ice velocity of the glaciers in the study area during 2000 and 2020 draped on the hill shade map.

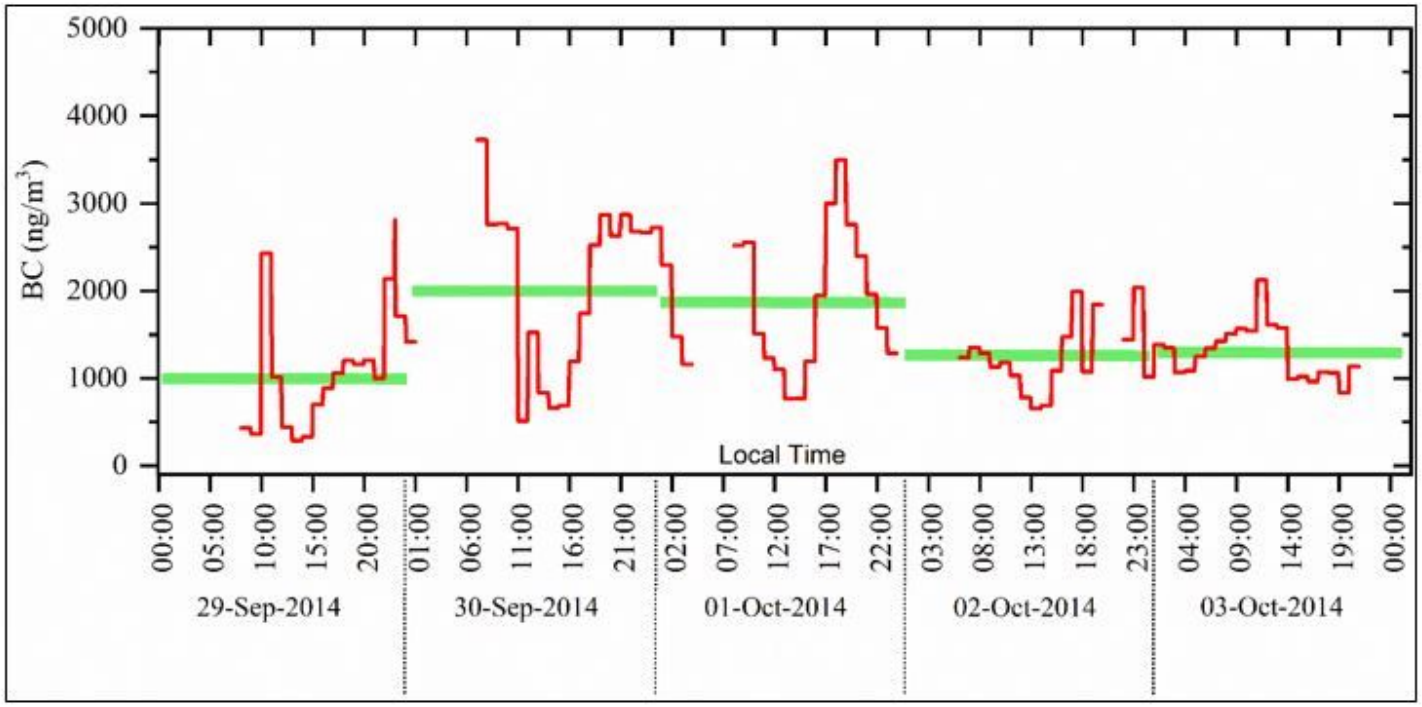

Figure 5

In-situ BC concentration observations near the ablation zone of the Machoi Glacier in the study area.

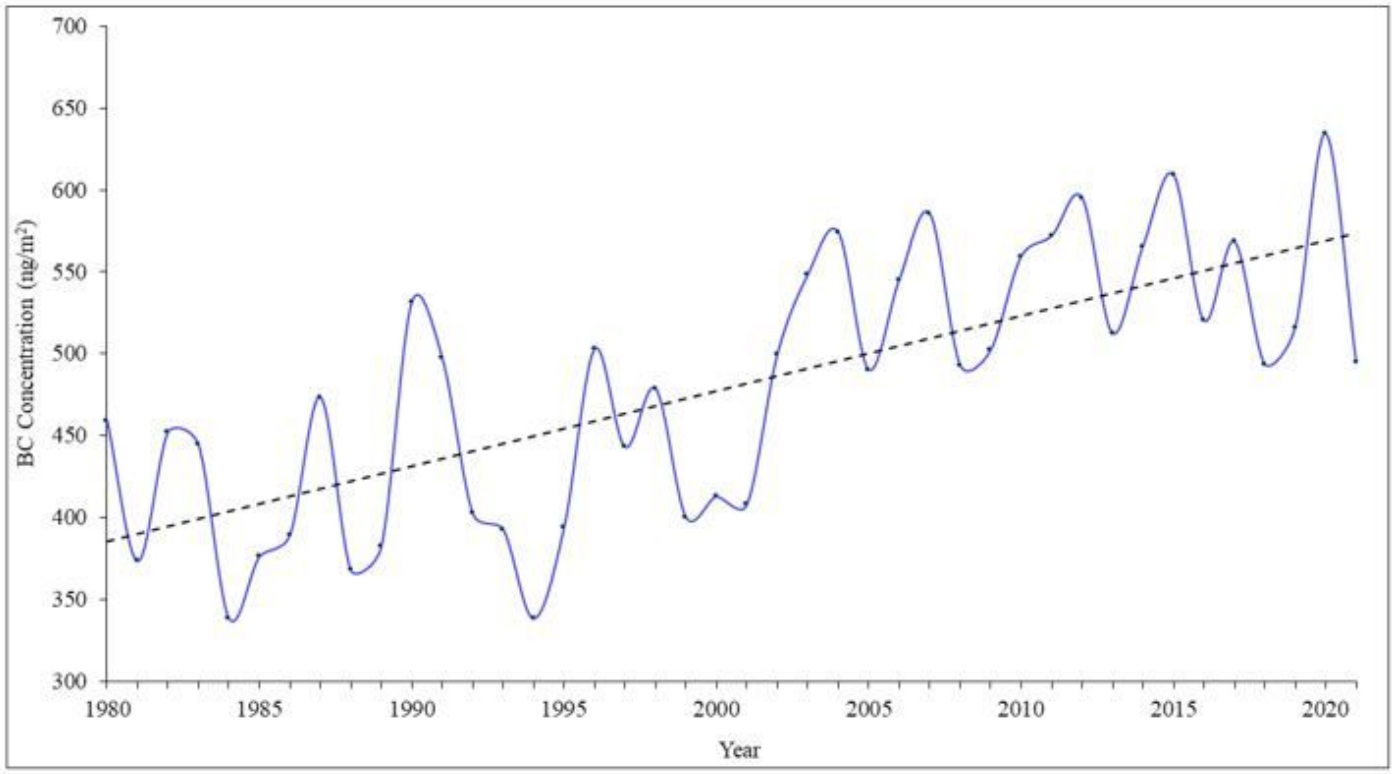

Figure 6

Area-averaged MERRA reanalysis BC mass concentration data in the study area from 1980 to 2020

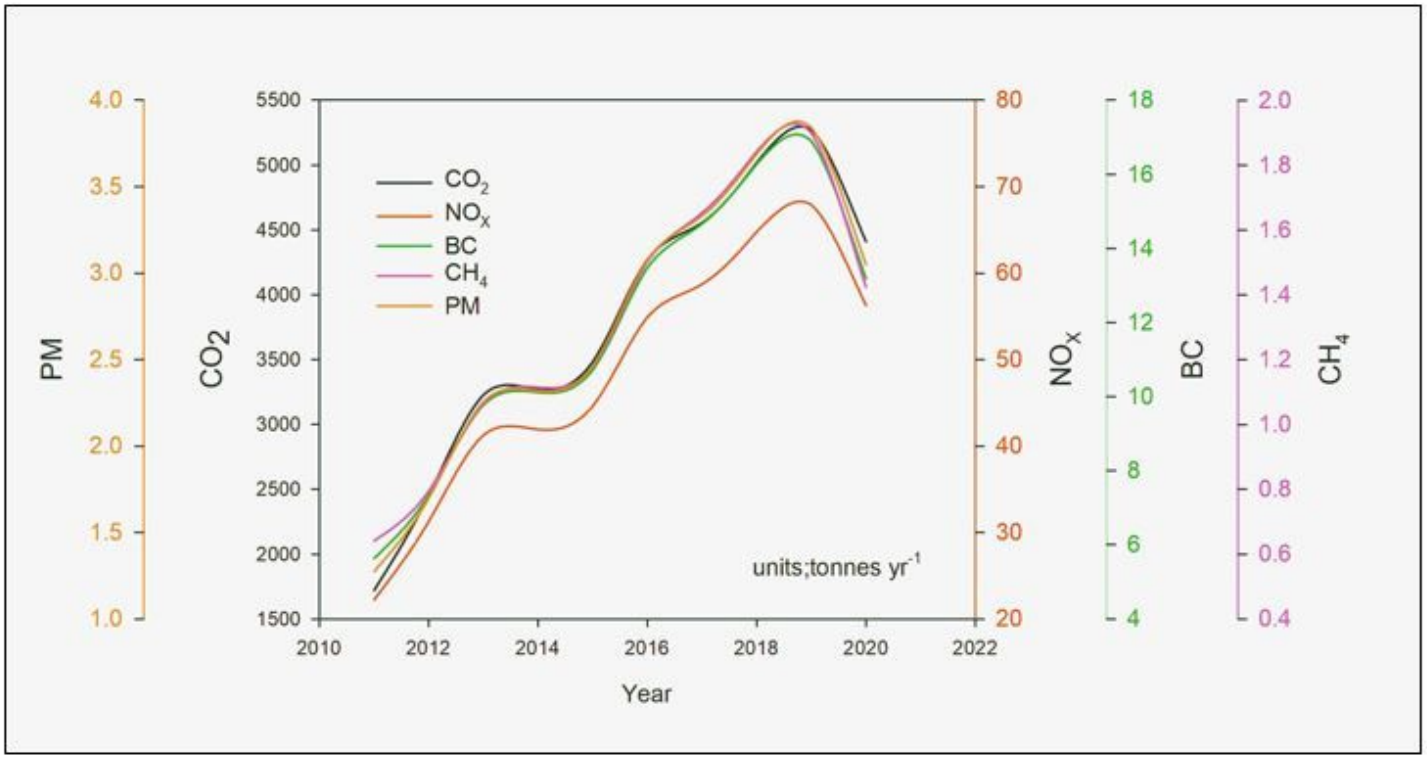

Figure 7

PM, CO2, NO_x, BC and CH_4 emissions (tonnes/year) emitted from the vehicular traffic plying on the national highway passing in the vicinity of the glaciers in study area.

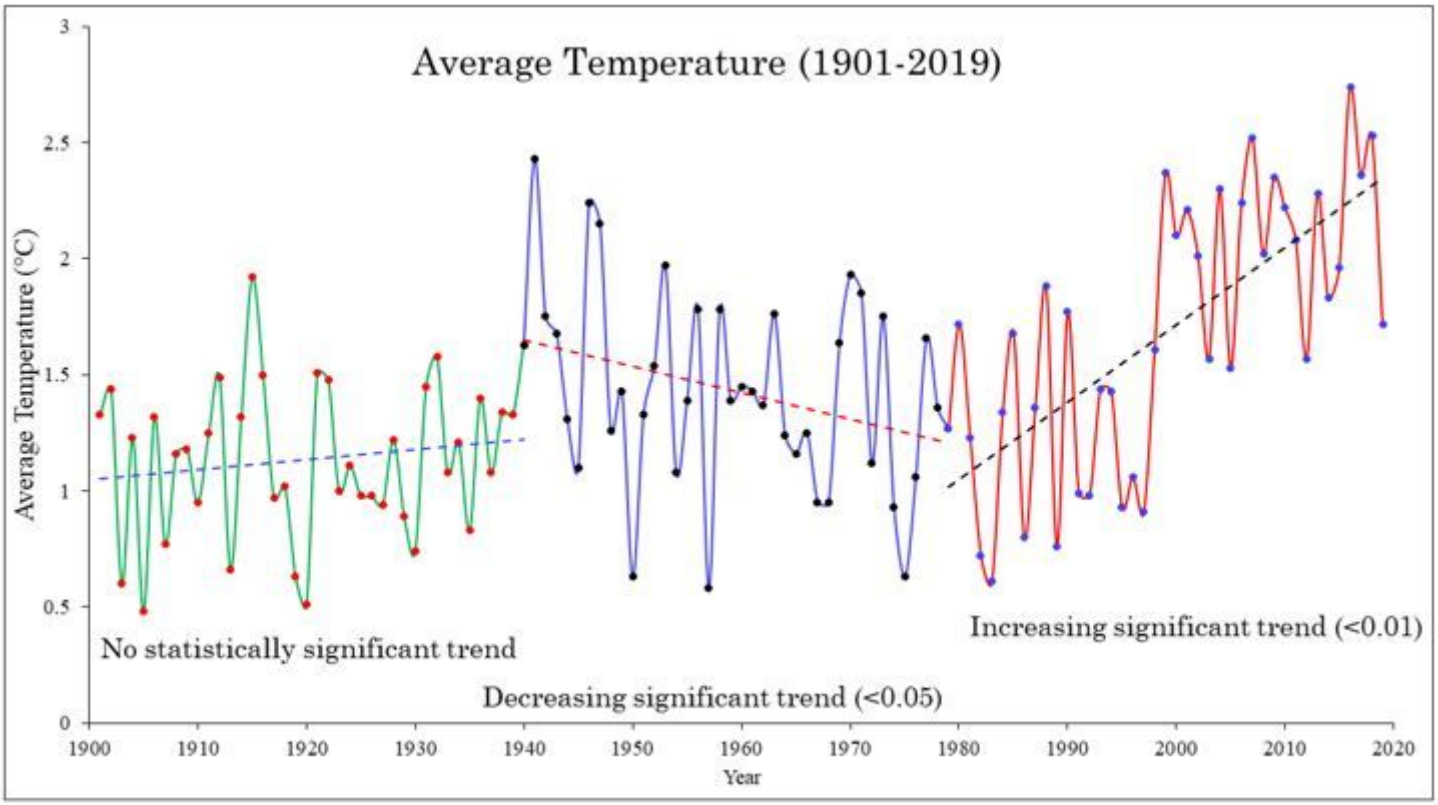

Figure 8

Annual average temperature of the study area from 1901–2019 derived from the CRU data. Dashed line represents the linear trend.

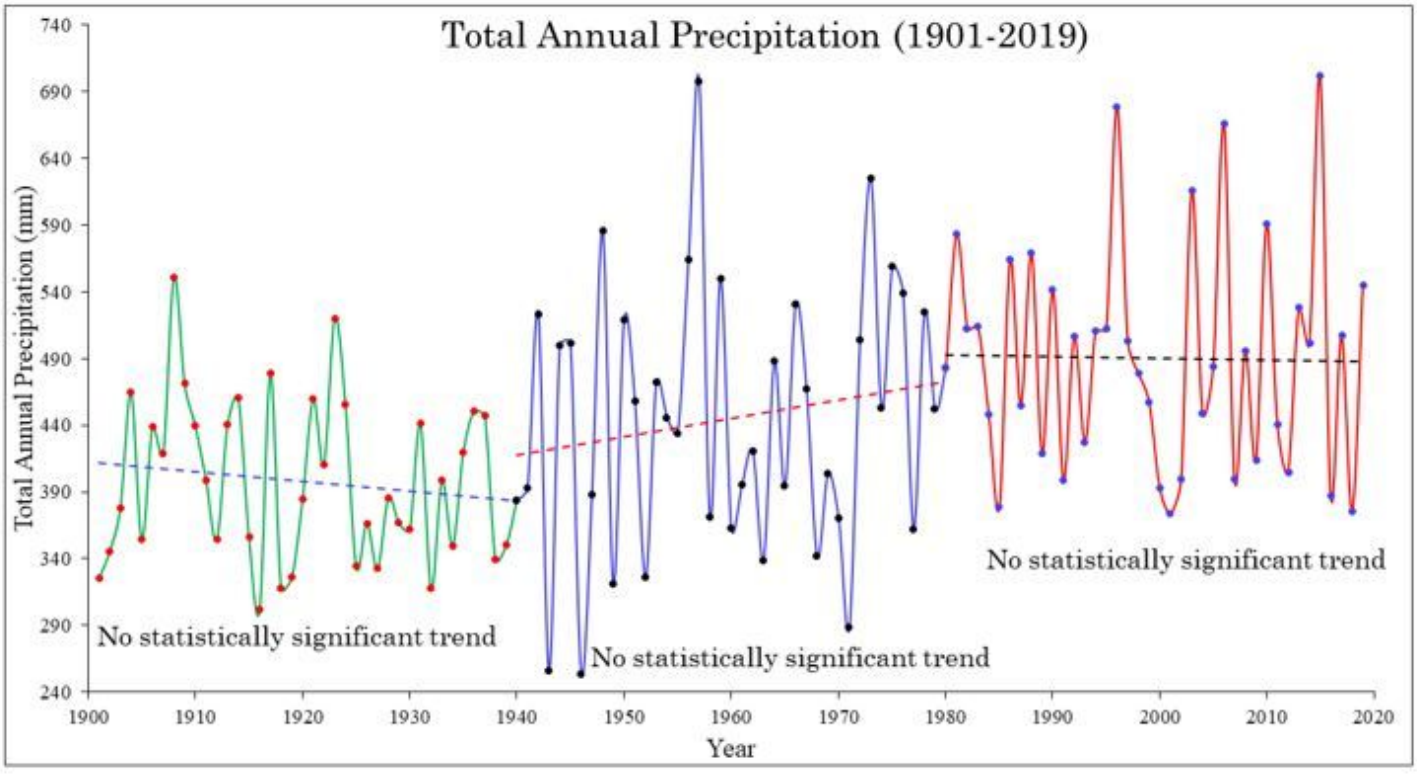

Figure 9

Annual variability precipitation of the study area from 1901-2019 derived from the CRU climate data. Dashed line represents the linear trend.

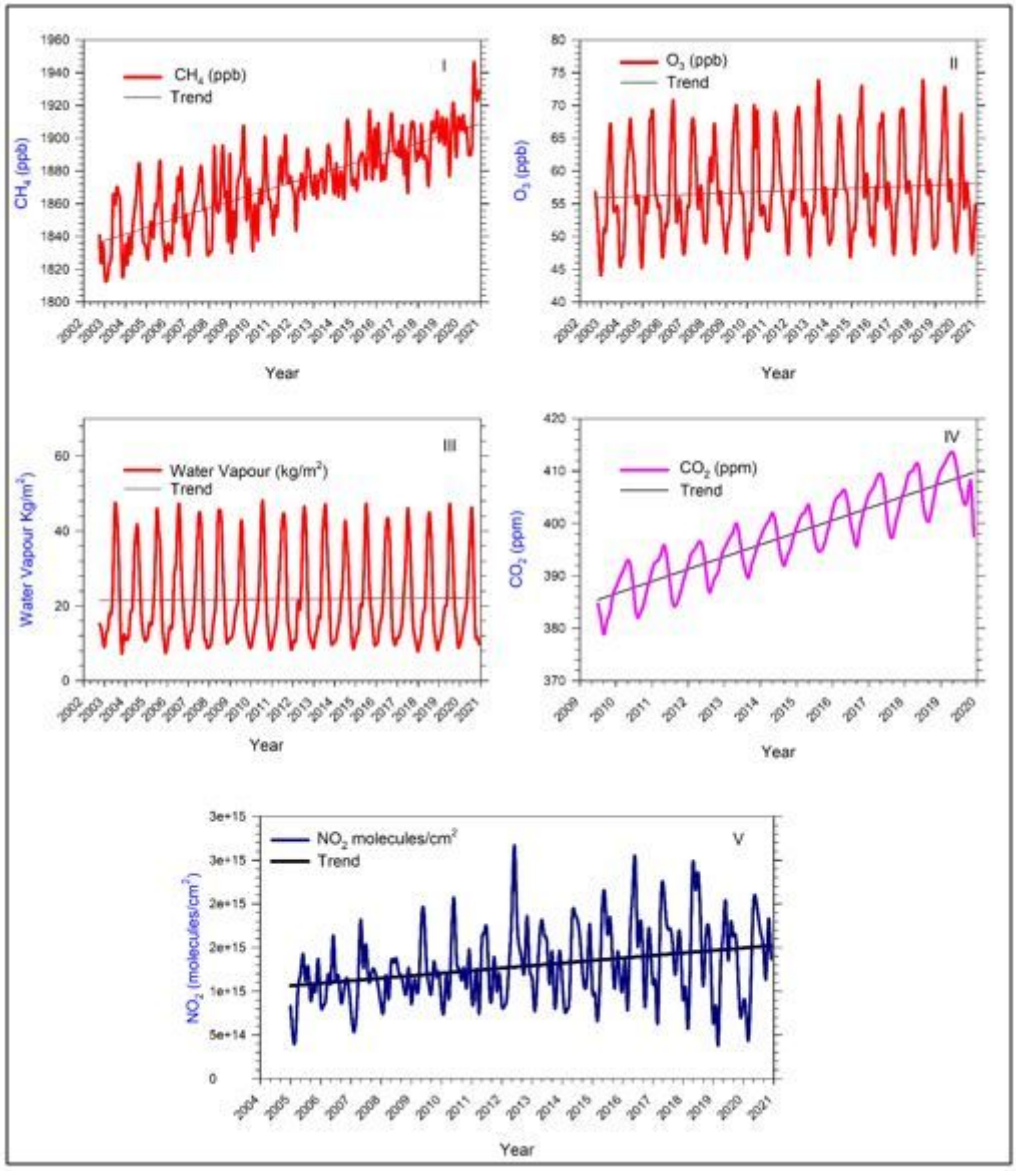

Figure 10

Temporal variation of the various GHGs concentration extracted from various satellites over the study area; I) Monthly variation of CH_4 from 2003 to 2020, II) Monthly variation of O_3 from 2003 to 2020, III) Monthly variation of Water vapor from 2003 to 2020, IV) Monthly variation of CO_2 from 2009 to 2019 and V) Monthly variation of NO_2 from 2005 to 2020.

Supplementary Files

This is a list of supplementary files associated with this preprint. Click to download.

- Supplementary.docx